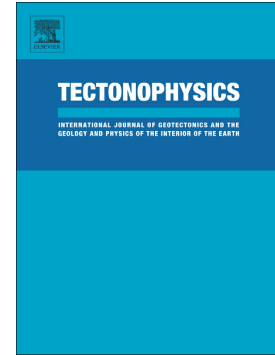


Accepted Manuscript

Jurassic high heat production granites associated with the Weddell Sea rift system, Antarctica

Philip T. Leat, Tom A. Jordan, Michael J. Flowerdew, Teal R. Riley, Fausto Ferraccioli, Martin J. Whitehouse



PII: S0040-1951(17)30464-X
DOI: doi:[10.1016/j.tecto.2017.11.011](https://doi.org/10.1016/j.tecto.2017.11.011)
Reference: TECTO 127677
To appear in: *Tectonophysics*
Received date: 8 May 2017
Revised date: 31 October 2017
Accepted date: 6 November 2017

Please cite this article as: Philip T. Leat, Tom A. Jordan, Michael J. Flowerdew, Teal R. Riley, Fausto Ferraccioli, Martin J. Whitehouse , Jurassic high heat production granites associated with the Weddell Sea rift system, Antarctica. The address for the corresponding author was captured as affiliation for all authors. Please check if appropriate. Tecto(2017), doi:[10.1016/j.tecto.2017.11.011](https://doi.org/10.1016/j.tecto.2017.11.011)

This is a PDF file of an unedited manuscript that has been accepted for publication. As a service to our customers we are providing this early version of the manuscript. The manuscript will undergo copyediting, typesetting, and review of the resulting proof before it is published in its final form. Please note that during the production process errors may be discovered which could affect the content, and all legal disclaimers that apply to the journal pertain.

Jurassic High Heat Production granites associated with the Weddell Sea rift system, Antarctica

Philip T. Leat^{a,b}, Tom A. Jordan^a, Michael J. Flowerdew^{a,c}, Teal R. Riley^a,
Fausto Ferraccioli^a, Martin J. Whitehouse^d

^a British Antarctic Survey, High Cross, Madingley Road, Cambridge CB3 0ET, UK

^b Department of Geology, University of Leicester, University Road, Leicester LE1 7RH, UK

^c CASP, West Building, Madingley Rise, Madingley Road, Cambridge CB3 0UD, UK

^d Swedish Museum of Natural History, Box 50007, SE-104 05, Stockholm, Sweden

E-mail addresses:

PT Leat: ptle@bas.ac.uk

TA Jordan: tomj@bas.ac.uk

MJ Flowerdew: Michael.flowerdew@casp.cam.ac.uk

TR Riley: trr@bas.ac.uk

F Ferraccioli: ffe@bas.ac.uk

MJ Whitehouse: martin.whitehouse@nrm.se

Corresponding author: Philip Leat: ptle@bas.ac.uk

Abstract

The distribution of heat flow in Antarctic continental crust is critical to understanding continental tectonics, ice sheet growth and subglacial hydrology. We identify a group of High Heat Production granites, intruded into upper crustal Palaeozoic metasedimentary sequences, which may contribute to locally high heat flow beneath the West Antarctic Ice Sheet. Four of the granite plutons are exposed above ice sheet level at Pagano Nunatak, Pirrit Hills, Nash Hills and Whitmore Mountains. A new U-Pb zircon age from Pirrit Hills of 178.0 ± 3.5 Ma confirms earlier Rb-Sr and U-Pb dating and that the granites were emplaced approximately coincident with the first stage of Gondwana break-up and the developing Weddell rift, and ~ 5 m.y. after eruption of the Karoo-Ferrar large igneous province. Aerogeophysical data indicate that the plutons are distributed unevenly over 40000 km^2 with one intruded into the transtensional Pagano Shear Zone, while the others were emplaced within the more stable Ellsworth-Whitmore mountains continental block. The granites are weakly peraluminous A-types and have Th and U abundances up to 60.7 and 28.6 ppm respectively. Measured heat production of the granite samples is $2.96\text{-}9.06 \text{ } \mu\text{W}/\text{m}^3$ (mean $5.35 \text{ W}/\text{m}^3$), significantly higher than average upper continental crust and contemporaneous silicic rocks in the Antarctic Peninsula. Heat flow associated with the granite intrusions is predicted to be in the range $70\text{-}95 \text{ mW}/\text{m}^2$ depending on the thickness of the high heat production granite layer and the regional heat flow value. Analysis of detrital zircon compositions and ages indicates that the high Th and U abundances are related to enrichment of the lower-mid crust that dates back to 200-299 Ma at the time of the formation of the Gondwanide fold belt and its post-orogenic collapse and extension.

Keywords: West Antarctica, heat flow, geothermal flux, A-type granite, continental rift

1. Introduction

The distribution and magnitude of geothermal heat flow in Antarctica is important for understanding lithospheric evolution and tectonic and mantle processes (Shapiro and Ritzwoller, 2004; Carson et al., 2014; Ramirez et al., 2016). It is also important for its influence on ice sheet growth, current and ancient subglacial processes and their influence on glacier flow (Pollard and DeConto, 2003; Pollard et al., 2005; Llubes et al., 2006).

Nevertheless, variations in geothermal heat flux under both East and West Antarctic ice sheets (Fig. 1) are poorly known (e.g. Carson et al., 2014; Ramirez et al., 2016). There are few direct measurements of heat flow in Antarctica; borehole measurements in the Ross Sea area are as high as 115 mWm^{-2} at the ANDRILL borehole site (Fig. 1) but this is in close proximity to the Erebus Volcanic Province (Morin et al., 2010), and considerably above the average for the continent, which is thought to be approximately 65 mWm^{-2} , close to the global continental average (Fox-Maule et al., 2005). Regional values used in glaciological models are often based on values from tectonic terranes of similar crustal age in other parts of the world. This has led to heat flow values of about $37\text{-}55 \text{ mWm}^{-2}$ being used in the models for Archaean-Proterozoic East Antarctica, and higher values of about $60\text{-}85 \text{ mWm}^{-2}$ for West Antarctica, in view of its history of Mesozoic-Cenozoic magmatism and rifting (e.g. Pollard et al., 2005; Llubes et al., 2006). The significantly higher estimates for heat flow in West relative to East Antarctica are supported by analysis of seismic data. Ritzwoller et al. (2001) used seismic data to estimate lithospheric temperatures beneath the continent, and showed higher heat flux beneath West Antarctica than beneath the relatively stable East Antarctica. Lithospheric heat flow derived from a global seismic model was modelled for Antarctica by Shapiro and Ritzwoller (2004) who again showed elevated temperatures in parts of West Antarctica, where heat flow values above 100 mW/m^{-2} were suggested. Furthermore, interpretation of satellite-derived magnetic data by Fox Maule et al. (2005) indicated higher heat flow in parts of West Antarctica and along the Transantarctic Mountains than in East Antarctica. More recent seismic estimates of geothermal heat flux suggest values of $62\text{-}74 \text{ mW/m}^{-2}$ in the West Antarctic rift system but $58\text{-}62 \text{ mW/m}^{-2}$ in the Ellsworth-Whitmore mountains region (An et al., 2015a).

There is increasing evidence for local high heat flow ‘hot spots’ in Antarctica. In West Antarctica, these are mainly thought to reflect volcanic heating and may cause enhanced glacial basal melting (Schroeder et al., 2014). However, they can also be caused by local areas with high heat production lithologies. Carson et al. (2014) calculated that crustal heat production and heat flow are variable in the Prydz Bay area of East Antarctica due to the presence of high heat production granite, and locally 2-3 times higher than the values normally assumed for East Antarctica. Burton-Johnson et al. (2017) concluded that upper crustal heat production and heat flow in the Antarctic Peninsula are more variable than modelling based on geophysical data suggest.

In this paper, we examine a region of Antarctica that has potential high heat flow due to the occurrences of Mesozoic granites. The granites have high heat production and were intruded into the upper crust coincident with the development of the Weddell Sea rift system (Fig. 1). The high heat production (HHP) granites are exposed in the Ellsworth-Whitmore terrane (Figs. 1, 2a), in the region of onset of enhanced glacial flow for several major ice streams, including the Institute and Möller flowing towards the Weddell Sea (Bingham and Siegert, 2007; Ringot et al., 2011), and also some of the dynamic ice streams flowing to the Siple Coast (e.g. Payne 1998). The HHP granites lie upstream of both ancient subglacial melt water channels (Rose et al., 2014), and of several dynamic subglacial lakes identified by satellite observations (Fig. 2a) (Smith et al., 2009; Siegert et al., 2014). Although heat flow has not been directly measured in the vicinity of the granites, their high heat production values suggest elevated surface heat flow should be expected. As a consequence, heat flow resulting from basement lithologies may have significantly more local variability than implied by regional values based on tectonic age or continental scale geophysical models, with potential implications for glaciological modelling.

2. Ellsworth-Whitmore terrane

The granites intrude the Ellsworth-Whitmore terrane (Craddock et al., 2017), an elevated region of central West Antarctica that forms most of a sub-ice topographical ridge known as the

Ellsworth Mountains-Thiel Mountains ridge (Storey and Dalziel, 1987). This ridge bisects West Antarctica and underlies the ice divide between the Weddell Sea and the Siple Coast and Amundsen Sea catchments (Figs. 1, 2a). The granite outcrops are situated at Whitmore Mountains and in scattered mountains and nunataks to the east (Fig. 2a). Aerogeophysical data and geological comparisons have been employed to conclude that the Ellsworth-Whitmore terrane is underlain by one of the main crustal blocks of West Antarctica which moved relative to one another during Mesozoic deformation. Most authors have included the Whitmore Mountains, and other mountains and nunataks where the granites crop out, within the Ellsworth-Whitmore mountains crustal block, and the block is also thought to include the region of basement exposed at Haag Nunataks (Grunow et al., 1987; Storey et al., 1988a; Maslanyj and Storey, 1990; Curtis and Storey, 1996; Jordan et al., 2017). The crustal block separates the Jurassic Weddell Sea rift system to the east from the Cretaceous and more recent West Antarctic rift system to the west (Fig. 1).

In the Ellsworth Mountains, a 13 km thick Cambrian to Permian sedimentary succession is exposed (Weber et al., 1992; Curtis, 2001; Flowerdew et al., 2006) with a conformable Cambrian volcanic succession near its base (Curtis et al., 1999). The granites are intruded into dominantly siliciclastic metasedimentary rocks thought to correlate with this sedimentary succession (Storey and Dalziel, 1987). The metamorphic grade of the metasedimentary group is generally low, with a single high-grade paragneiss locality at Mount Wollard (Storey and Dalziel, 1987).

Crust underlying this Palaeozoic succession is not exposed in the Ellsworth-Whitmore terrane, but is thought to be similar to Mesoproterozoic gneisses exposed at Haag nunataks (Curtis and Storey, 2006), and aeromagnetic data are interpreted to suggest that this Proterozoic crust underlies the northeastern margin of the terrane (Maslanyj and Storey, 1990; Jordan et al., 2017). Gneisses from the Haag block have been Rb-Sr dated at 1176 ± 76 Ma and are cut by minor granitic intrusions Rb-Sr dated at ~ 1060 -1000 Ma (Millar and Pankhurst, 1987). Nd isotopic compositions of Cambrian volcanic rocks in the Ellsworth Mountains and the Jurassic granites in the Ellsworth-Whitmore terrane are consistent with Mesoproterozoic crust and

lithospheric mantle underlying much of the terrane (Pankhurst et al., 1991; Curtis et al., 1999; Millar et al., 2001; Leat et al., 2005).

3. Weddell Sea rift system

The Weddell Sea rift system is situated on the continental lithosphere of Antarctica (Fig. 1). The eastern margin of the rift exposes Proterozoic to Early Palaeozoic lithologies in Coats Land, the Pensacola Mountains and Thiel Mountains (Storey and Dalziel, 1987; Dalziel, 1991; Veevers, 2012) and is roughly coincident with the margin of the relatively stable East Antarctic lithosphere (Studinger and Miller, 1999; An et al., 2015b). The western margin of the rift follows the eastern margins of the Antarctic Peninsula, Haag and Ellsworth-Whitmore mountains crustal blocks. All these blocks are interpreted to have moved away from East Antarctic as the Weddell Sea rift extended during the Mesozoic break-up of Gondwana (Fig. 2b), with the Ellsworth-Whitmore terrane and Haag blocks also having been rotated (Storey et al., 1988a; Grunow et al., 1991; Curtis and Storey, 1996; King et al., 1996; Curtis, 2001; Randall and Mac Niocaill, 2004).

According to interpretations of recent aerogeophysical data (Jordan et al., 2013) the rift is some 400-600 km wide along most of its length, narrowing to the south, and extends some 900 km from its inland termination against the Ellsworth-Whitmore mountains block to the Antarctic continental margin where it widens to form the Weddell Sea embayment (King, 2000).

Extension was unevenly distributed in the rift, and probably was strongest in the central basins. East-West extension within the rift system was accommodated by movement along the Pagano Shear Zone (Fig. 2a), which is interpreted a left-lateral transtensional structure (Jordan et al., 2013). Crustal thickness in the Weddell rift is reported to be as thin as 29 km according to estimates from gravity data derived from the GRACE satellite (Block et al., 2009), in agreement with earlier estimates of 27-29 km using marine and land gravity data in the Weddell embayment (Studinger and Millar, 1999). These are among the thinnest estimated crustal thicknesses in continental Antarctica (Block et al., 2009), and are striking when considering

seismic data that indicates that as much as 15 km of syn- to post rift sediment may be present within the rift (Leitchenkov and Kudryavtzev, 1997). Jordan et al. (2017) divided the Weddell Sea rift system into a Northern Weddell Magnetic Province dominated by magnetic anomalies with a NE-SW trend, and a Southern Weddell Magnetic Province with approximately N-S trending magnetic anomalies, which is the part of the rift system adjacent to the Ellsworth-Whitmore terrane and associated with the granites (Fig. 3b). The large N-S magnetic anomalies in the southern province are interpreted to reflect dominantly igneous rocks controlled by major rift faults and contemporaneous with the Jurassic extension (Jordan et al., 2017). Cross-cutting relationships of magnetic anomalies suggest that the southern province represents an earlier phase in the development of the Weddell Sea rift system than the northern province (Fig. 2b) (Jordan et al., 2017). Seismic and gravity interpretations further suggest that the lowermost crust of Weddell Sea rift system comprises a dense, high-velocity layer interpreted to be mafic intrusions (underplate) locally up to ca. 10 km thick (Leitchenkov and Kudryavtzev, 1997; King, 2000; Jordan et al., 2013; Jordan et al., 2017).

The age of extension in the Weddell rift has not been dated directly but is thought to be dominantly Early-Middle Jurassic in age, coincident with the initial phases of Gondwana break-up, based on structural data and tectonic reconstructions (Storey et al., 1988a; Grunow et al., 1991; Dalziel et al., 2013; Jordan et al., 2013; Jordan et al., 2017). This age for the extension is approximately consistent with estimates of lithosphere thermal age between 165 and 230 Ma (Studinger and Millar, 1999). There is no evidence of significant post-Jurassic rifting in the Weddell rift (Studinger and Millar, 1999; King and Bell, 1996).

4. The Ellsworth-Whitmore granites

There is good coverage of aerogravity and aeromagnetic data over the southern Weddell Sea rift system and the Ellsworth-Whitmore terrane (Garett et al., 1988; Jordan et al., 2013; Jordan et al., 2017). Interpretations of gravity and magnetic anomalies indicate that igneous intrusions are distributed unevenly across some 40 000 km² of the region and form an igneous province of significant volume (Jordan et al., 2013). The aerogeophysical data including sub-ice topography

and aeromagnetic anomaly maps of the Pirrit hills, Nash Hills and Pagano Nunatak are presented in Fig. 3. These show the granite outcrops at Pirrit Hills, Nash Hills and Pagano Nunatak are all associated with significant magnetic anomalies of 60-300 nT. The geophysical data suggest that the granites are associated with broad highlands, and are much more extensive than the outcrops suggest. Additional smaller non-exposed intrusions are also inferred between Nash Hills and Pagano Nunatak.

4.1 Pirrit Hills

The Pirrit Hills granite is exposed across a range of peaks and outlying nunataks forming an outcrop some 18 km across centred on 81°17'S, 85°21'W (Lee et al., 2012; Craddock et al., 2017), ~50 km SW of the >2000 m deep Ellsworth Trough. A large positive magnetic anomaly with an amplitude of up to 290 nT and a wavelength of ca. 50 km (Jordan et al., 2013) is centred on the granite outcrop (Fig. 3b). Garrett et al. (1988) modelled the intrusion to be ca. 18 km thick and a composite body, consisting of a granitic upper part and a gabbroic base in approximately equal proportions. However, the granite is not associated with any significant positive Bouguer gravity anomaly, suggesting that the granite is not directly underlain by a significant volume of gabbroic material (Jordan et al., 2013).

4.2 Nash and Martin hills

The Nash Hills granite is exposed in the Nash Hills at 81°53'S, 89°23'W, forming a range some 2 km across. The Martin Hills are approximately 25 km to the southeast and the granite outcrops have been suggested to be a continuation of the same granite intrusion (Pankhurst et al., 1991; Craddock et al., 2017). A positive magnetic anomaly of ca. 60 nT with a wavelength of some 50 km is coincident with the Nash and Martin hills, consistent with the area being underlain by a single large granite intrusion (Jordan et al., 2013) as modelled in Fig. 4. Garrett et al. (1988) modelled the magnetic data to suggest a ca. 12 km thick intrusion consisting of granite overlying gabbro. However, there is no positive Bouguer anomaly associated with the intrusion (Fig. 4b). The pluton was re-modelled (Jordan et al., 2013) as up to 8 km thick with no shallow

gabbroic layer (Fig. 4c). However, an underplated layer of dense mafic material at the base of the crust would be consistent with the observed long wavelength gravity anomalies in this region (Fig. 4c).

4.3 Pagano Nunatak

The granite at Pagano Nunatak forms a 0.8 km long, 23 m high cliff-like outcrop at 83°41'S, 87°40'W (Webers et al., 1983; Craddock et al., 2017). This granite is associated with a large positive magnetic anomaly of up to 246 nT, some 50 km wide and 125 km long with a NE-SW trend (Fig. 3). The Pagano anomaly is strikingly linear and forms the southern margin of the wider Pagano shear zone, a major fault system at least 800 km long identified from aerogeophysical data. The Pagano shear zone is thought to be a sinistral transtensional fault along which the Ellsworth-Whitmore crustal block was translated away from the East Antarctic margin, accommodating extension within the Weddell Sea rift system (Jordan et al., 2013; Jordan et al., 2017). Between Pagano Nunatak and Nash Hills, a series of *en-echelon* basins form part of the shear zone (Fig. 3a) and are associated with smaller positive magnetic anomalies interpreted as additional granite plutons (Figs. 3b, 4). Garrett et al. (1988) modelled the Pagano Nunatak intrusion as a composite granite-gabbro pluton up to ca. 18 km thick. As no positive Bouguer gravity anomaly is associated with the pluton, it is re-modelled as a granitic body ~8 km thick (Jordan et al., 2013; Fig. 4). The large resulting volume of the Pagano Nunatak granite, and its orientation along the Pagano shear zone, suggest that it was potentially intruded in a transtensional releasing bend in the active shear zone. In contrast, the other major granites have no clearly defined preferred orientation, suggesting they were emplaced within the relatively stable and non-deforming core of the Ellsworth-Whitmore mountains block.

4.4 Whitmore Mountains

In the Whitmore Mountains there are two distinct granites (Pankhurst et al., 1991). The Triassic age Mount Seelig granite crops out in several nunataks including Mount Seelig, Mount Chapman and Linck Nunataks. The intrusion is at least 25 km across, and centred on 82°30'S,

104°30'W (Webers et al., 1982). The Jurassic Linck Nunataks granite crops out at Linck Nunataks and at Mount Chapman, forming an outcrop 25 km across centred at 82°37'S, 105°00'W (Webers et al., 1982; Vennum and Storey, 1987). It intrudes the Mount Seelig granite as dykes (Webers et al., 1982). Geophysical data coverage in this area is sparse, but neither of these granites appears to be associated with significant magnetic or gravity anomalies (Jordan et al., 2013) and the thicknesses of the plutons have not been modelled from geophysical data.

4.5 Summary of previous petrological and geochemical investigations

The exposed granites are massive, leucocratic, and show no obvious indications of deformation, consistent with Mesozoic rifting being the last significant tectonic event in the Weddell rift.

They range in composition from granodiorite to granite (s.s.) (Craddock et al., 2017).

Petrographically, the granites at Pagano Nunatak, Pirrit Hills and Nash Hills are dominantly medium to coarse grained and contain abundant alkali feldspar megacrysts up to 3-4 cm long (Webers et al., 1982, 1983; Vennum and Storey, 1987). The Linck Nunataks granite is finer-grained and more equigranular with feldspars up to 1 cm long (Lee et al., 2012). The granites typically consist of alkali feldspar, quartz, plagioclase, biotite and muscovite, with minor or trace amounts of Fe-oxides, apatite and zircon (Vennum and Storey, 1987; Lee et al., 2012). They are therefore two-mica granites and are typical of two-mica granites globally (Lee et al., 1981; Vidal et al., 1982; Charoy, 1986). Aplite and granite dykes and pegmatites containing tourmaline, beryl, muscovite and garnet are reported from the granites (Weber et al., 1983; Vennum and Storey, 1987; Craddock et al., 2017). The older Mount Seelig granite is different, composed of quartz, alkali feldspar plagioclase, biotite and amphibole (Webers et al., 1982).

The Ellsworth-Whitmore terrane granites have been dated by several isotopic methods. All of the intrusions have been dated by precise U-Pb isotope analysis of zircon separates, establishing that the Pirrit Hills granite, Linck Nunataks granite, Pagano Nunatak granite and the Nash Hills granite are all Jurassic in age (Lee et al., 2012; Craddock et al., 2017). These U-Pb data confirm the Jurassic ages for the granites suggested by earlier K-Ar and R-Sr isotope work (Weber et al., 1982, 1983; Millar and Pankhurst, 1987; Pankhurst et al., 1991). In the Whitmore

Mountains, the Permian age (200 ± 5 Ma U-Pb age) Mount Seelig granite is distinct from the Jurassic age Linck Nunataks granite (Pankhurst et al., 1991; Craddock et al., 2017).

Several studies have emphasized that the granites are petrogenetically distinct within the context of West Antarctica, having S-type, high-Al saturation characteristics (Millar and Pankhurst, 1987; Storey et al., 1988b; Pankhurst et al., 1991), and Vennum and Storey (1987) contrasted them to the dominantly I-type, less Al-saturated granites along the Pacific margin of Antarctica. The origin of the Ellsworth-Whitmore terrane granites has been proposed to be either largely by melting of continental crust (Millar and Pankhurst, 1987; Vennum and Storey, 1987; Millar et al., 2012; Lee et al., 2012) or by a combination of crustal melting and fractionation from basaltic magma similar in composition to Jurassic age Ferrar magmas (Storey et al., 1988b; Pankhurst et al., 1991; Craddock et al., 2017). However, Millar et al. (2001) argued, on the basis of Oxygen isotope data, that a contribution from mafic magmas similar to Ferrar basalts cannot be detected in the granites. Most authors have agreed that the heat required for the crustal melting to generate the granite magmas was provided by contemporaneous Ferrar magmatism or closely related Jurassic magmas intruded into the Weddell Sea rift system during Jurassic-age extension (Storey et al., 1988b; Pankhurst et al., 1991; Craddock et al., 2017).

5. Methodology

The paper combines new and compiled published geochronological and geochemical data from the Ellsworth-Whitmore terrane granites with published geophysical data to comment on their tectonic relationships, heat production and potential contribution to surface heat flow.

Zircons from sample V48A, a granite from Pirrit Hills (Storey et al., 1988b), were separated from coarse crush and analysed for U-Pb geochronological determination using a Cameca 1270 ion-microprobe housed at the NORDSIM facility, Swedish Museum of Natural History. Methods followed those of Whitehouse and Kamber (2005).

New major and trace element determinations were carried out on nine samples from the Pagano Nunataks, Nash Hills, Mount Chapman and Pirrit Hills granites (sample locations and

descriptions in Supplementary Material). Samples were crushed in a Tungsten Carbide (WC) mill. Major elements were determined by standard XRF methods at the Department of Geology, University of Leicester, UK, and trace elements by ICP-MS at Department of Geological Sciences, University of Durham, UK. These represent, along with those presented by Lee et al. (2012) for the Pirrit Hills granite, the first published precise trace element determinations by ICP-MS for the granite group.

6. Results

6.1 *U-Pb Geochronology*

Results of the ion-microprobe analysis of separated zircons in Pirrit Hills granite sample V48A are presented in Table 1 and Fig. 5. CL and secondary electron (SE) images of the zircons indicating analysed spots are presented in Supplementary Material. Points plotting above the concordia in Fig. 5 contain appreciable common Pb and are not included in the age calculation. Several of the points had high U abundances of more than 4000 ppm, suggesting that damage to the zircon structure might have occurred due to radiogenic decay, and also have high common Pb contents. Grains with such high U contents are likely to yield erroneously old SIMS ages (White and Ireland, 2012) and will also be more susceptible to episodes of post-magmatic Pb loss. The remaining four points form a tight, overlapping cluster along the concordia and define a concordia age of 178.0 ± 3.5 Ma (Fig. 5). This is taken as the age of intrusion of the pluton. There is no evidence in the new data for significant inheritance of zircons.

6.2 *Geochemistry*

The major and trace element analyses are presented in Table 2. Ta abundances are not reported as they may have been contaminated during crushing in WC. To explore geochemical variations in the granites, we also use geochemical data previously reported for the Pirrit Hills granite by Lee et al. (2012) and for all of the granites by Vennum and Storey (1987) and Storey et al. (1988b).

7. Discussion

7.1 Age relationships

The new ion-microprobe zircon U-Pb age of 178.0 ± 3.5 Ma is interpreted as closely representing the age of emplacement of the Pirrit Hills granite. This granite has been previously dated as 176 ± 5 Ma by K-Ar, and 173 ± 3 Ma by Rb-Sr whole-rock isochron (Millar and Pankhurst, 1987; Craddock et al., 2017). Lee et al. (2012) presented SHRIMP ion microprobe data on zircon separates suggesting an age of 164.5 ± 2.3 Ma for the granite. An older U-Pb SHRIMP zircon age of 168 ± 4 Ma was obtained for the intrusion by Craddock et al. (2017). Craddock et al. (2017) further presented U-Pb isotope dilution - thermal ionization mass spectrometry (ID-TIMS) data for zircon separates from two samples of the granite to give ages of 174.01 ± 0.14 and 174.06 ± 0.16 Ma, and suggested that these ID-TIMS ages are the best estimates for the age of crystallisation of the granite. Our ion-microprobe age is similar to these ages (older by a small margin), and the emplacement of the granite can be taken to be about 174-178 Ma. The significantly younger ages indicated by the two SHRIMP analyses may be a result of Pb loss due to radiation damage caused by the high U contents of zircons, as indicated by our data, and as suggested by Craddock et al. (2017). The U-Pb ages are within error of the K-Ar and Rb-Sr ages indicating no evidence for protracted cooling or resetting of the Ar and Rb-Sr systems beyond the errors in the K-Ar and Rb-Sr data.

This age is similar to those of the other Jurassic granites of the Ellsworth-Whitmore terrane. Preferred zircon U-Pb ages for the other granites are: Nash Hills, 177.4 Ma; Linck Nunataks, 174.8 Ma; Pagano Nunatak, 174.6 Ma (Craddock et al., 2017). These ages are within error of K-Ar and Rb-Sr ages (Webers et al., 1982; Millar and Pankhurst, 1987; Craddock et al., 2017), again indicating no evidence for protracted cooling. An exception is Nash-Martin Hills, where three granites yielded K-Ar ages of 163-167 Ma (Craddock et al., 2017), some 10-14 m.y. later than the U-Pb age. This is consistent with a greater degree of localised hydrothermal alteration of the sampled part of this granite.

The narrow 174-178 Ma range of intrusion ages of the granites is striking in view of the geographical spread of the outcrops within a complex rift system. The intrusions are more than 4 m.y. younger than the ages of both the Ferrar and Karoo parts of the large igneous province (LIP) erupted at the time of initiation of Gondwana break-up between southern Africa and Antarctica. Precise U-Pb data date the emplacement of the Ferrar magmas to 182.43 ± 0.036 to 182.779 ± 0.033 Ma (Burgess et al., 2015) and basaltic magmatism in the Karoo Basin to 182.3 ± 0.6 to 183.0 ± 0.5 Ma (Svensen et al., 2012). Younger Ar-Ar ages of 176.6 ± 1.8 Ma have been determined for the Ferrar magmatic province (Fleming et al., 1997). Nevertheless, the U-Pb data suggest that neither Karoo nor Ferrar magmas could have provided the heat source for crustal melting to form the Ellsworth-Whitmore terrane granites. The age of the granites is, however, within the range of the silicic volcanism and plutonism of the Chon-Aike silicic LIP recognised along the Pacific margin of Gondwana, including the Antarctic Peninsula and Thurston Island crustal blocks (Fig. 1; Pankhurst et al., 2000; Riley et al., 2017a; Riley et al., 2017b). The Ellsworth-Whitmore terrane granites are usually included in this LIP (Pankhurst et al., 1998; Pankhurst et al., 2000; Dalziel et al., 2013). The two early phases of Chon Aike volcanism (187-182 Ma and 172-162 Ma) straddle the age of the Ellsworth-Whitmore terrane granites. Generation of the silicic Chon Aike magmas likely occurred by partial melting of fertile lower crust along the active continental margin, at a time of lithospheric extension and generally enhanced mantle temperatures and mantle melting associated with the Karoo mantle plume (Pankhurst et al., 1998; Riley et al., 2001).

Evidence that the Pagano Nunatak granite was emplaced in a releasing bend in the Pagano shear zone suggests that this shear zone was active at 174.6 Ma (Craddock et al., 2017), and therefore that extension in the Weddell Sea rift system was also occurring at that time. It is possible that this lithospheric extension generated mafic magmatism forming a component of the thick lower crustal mafic underplate in the rift system, as well as heat for crustal melting. A component of the mafic underplate may also be magmas of the older (according to zircon U-Pb ages) Ferrar province which are thought to have been sourced within the early Weddell Sea rift system (Fleming et al., 1997; Elliot and Fleming, 2004).

7.2 Late-stage alteration

There is evidence for considerable late-stage hydrothermal veining and alteration in all of the granites. The Nash Hills granite is cut by both aplite dykes and quartz veins and the groundmass of the intrusion in Martin Hills has been extensively altered to sericite, carbonate and clay minerals (Vennum and Storey, 1987). The outcrop of the Pagano Nunatak granite is generally unaltered but it is cut by vuggy quartz veins up to 1 m wide which post-date aplite dykes (Webers et al., 1983; Vennum and Storey, 1987). The Pirrit Hills granite is variably altered from weak secondary sericite and chlorite development to locally strongly hydrothermally altered. It is cut by numerous veins of quartz-muscovite greisens (Vennum and Storey, 1987; Lee et al., 2012). The Linck Nunataks granite is generally fresh and is cut by aplite and pegmatite dykes (Webers et al 1982; Vennum and Storey, 1987).

The late magmatic, and alteration stages indicated by the widespread aplite and pegmatite dykes, veining and local pervasive alteration is comparable to the late-stage evolutions of other two-mica granite, tin-granite and HHP granite groups, which are commonly associated with extensive hydrothermal mineralization (e.g. Manning and Exley, 1984; Stone and Exley, 1985; Haapala, 1997), and is consistent with protracted late-stage cooling within the few m.y. allowed by the K-Ar and Rb-Sr geochronology. The evidence for late-stage hydrothermal alteration of the granites indicates that post-crystallisation mobilization of Na, K, Ca and other alkalis may have taken place, as we detail below.

7.3 Major element variation

Most of the analysed samples have <1.0 wt. % loss on ignition (LOI), and are relatively non-hydrated and fresh. Some samples from all the granites have 1-2 wt.% LOI and are moderately hydrated. One sample from the Martin Hills and one sample from Pirrit Hills have over 2 wt.% LOI. Pirrit Hills sample (P001-1) was identified as significantly altered by Lee et al. (2012) and is not discussed further. Pegmatite sample P005-3 has very low Zr (Lee et al., 2012), appears to be from a minor facies of the Pirrit Hills granite and is also excluded from both figures and discussion. Martin Hills sample (V24) is identified below as carbonated. As the more hydrated

and altered samples tend to form the outliers to the ranges, ranges and trends formed by the majority, less altered samples are quoted below.

Most of the samples have SiO_2 in the range 70.2-76.7 wt.%, and MgO in the range 0.03-0.84 wt.% and form a highly fractionated, silicic group. In the granites as a group, there is a clear inverse relationship between Si and Mg (Fig. 6a). CaO (range 0.43-1.8 wt.% in most samples) and total Fe as Fe_2O_3 (0.5-3.0 wt.%) are positively correlated with MgO and negatively correlated with SiO_2 (Fig. 6b, c). TiO_2 and P_2O_5 are similarly negatively correlated with SiO_2 (not shown). These relationships are consistent with the granites representing variable degrees of fractional crystallization of silicic melt involving removal of plagioclase, mafic minerals, Fe-Ti oxides and apatite. Three aplites shown in Fig. 6 fall compositionally within the granites, but toward low, more fractionated Mg, Ca and Fe abundances. Two granite samples (V24, Storey et al., 1988b; R.2230.7, Table 2) from the Martin Hills outcrops of the Nash Hills granite plot above the general SiO_2 - MgO and SiO_2 - CaO trends (Fig. 6a,c). The significantly higher abundances of Ca relative to Si strongly indicate that these samples have been altered by the addition of calcite, and the elevated Mg indicates that this is associated with dolomite as well. This is consistent with the identification of carbonate alteration of the Martin Hills granite outcrops by Vennum and Storey (1987).

Most of the samples have K_2O in the range 3.8-5.9 wt.% and Na_2O in the range 2.9-4.4 wt.%. K_2O is present in similar abundances in all the granites with a slight negative overall correlation with SiO_2 (Fig. 6d) and Na_2O shows a weak positive correlation with SiO_2 (not shown). According to Si-K relationships they have dominantly high-K compositions, transitional to medium-K.

The plot of $\text{K}_2\text{O}/\text{Na}_2\text{O}$ versus SiO_2 (Fig. 7a) illustrates that the $\text{K}_2\text{O}/\text{Na}_2\text{O}$ ratio of the granites varies significantly from around 1.1 to as low as 0.87 in the most fractionated Pirrit Hills and Nash Hills samples. The plot compares the Ellsworth-Whitmore terrane granites with widespread Triassic to Cretaceous, dominantly I-type, active continental margin granitoid plutons in the adjacent Antarctic Peninsula terrane (Fig. 1). The Ellsworth-Whitmore terrane granites have $\text{K}_2\text{O}/\text{Na}_2\text{O}$ ratios fully within the range of the Antarctic Peninsula ones. The figure also depicts the trend of potassic alteration common in silicic igneous rocks in which K increases

and Na is reduced during low-temperature processes, which appears to have affected several samples from the Antarctic Peninsula and Ellsworth-Whitmore terranes.

Fig. 7b shows aluminium saturation (molecular $Al/(Ca+Na+K)$) versus SiO_2 , again comparing the Ellsworth-Whitmore terrane granites with the Antarctic Peninsula ones. The Ellsworth-Whitmore terrane granites are entirely mildly peraluminous in having a small excess of Al over $(Ca+Na+K)$ by 1.00 to 1.11. However the figure illustrates that the Ellsworth-Whitmore terrane granites are no more peraluminous than the range of Antarctic Peninsula granitoids. In general, Antarctic Peninsula granitoids of Cretaceous age are I-type and are more metaluminous (molecular $Al/(Ca+Na+K) < 1$) and the Triassic and Jurassic granitoids are more peraluminous and S-like (Wever et al., 1995; Scarrow et al., 1996; Leat et al., 1997). In all age groups, Al saturation generally increases as SiO_2 increases, a function of crystal fractionation and assimilation of Al-oversaturated pelitic lithologies. The Ellsworth-Whitmore terrane granites have considerable overlap with all the age groups. The Ellsworth-Whitmore terrane granites cannot therefore be considered unusual in their Al saturation compared to granites of the Antarctic Peninsula active margin.

The S-type (derived by partial melting of continental crust of sedimentary origin) character of the granites was emphasized by Millar and Pankhurst (1987) and Vennum and Storey (1987). Storey et al. (1988b) pointed out that the granites are not classic cordierite-bearing S-types and emphasized their 'within-plate' continental rift setting association. Lee et al. (2012) proposed that the Pirrit Hills granites should be classified as A-type (anorogenic granite), a synonym for 'within-plate' granite, emphasising that it formed in a post-orogenic, rift setting with continental crust as the dominant source. The granites are post-orogenic with respect to the latest Palaeozoic to early Mesozoic Gondwanide orogeny (Dalziel et al., 2013), but their association with the developing highly magmatic Weddell Sea rift system probably dominated the magma genesis. The mildly peraluminous compositions of the granites indicates that melting of pelitic metasediments did not dominate their sources, despite their two-mica mineralogies. In the absence of other indications of classic S-type characteristics, it is probable that the A-type and 'within-plate' designations are correct, but it is noted that the granites are very different from alkaline A-types of continental rifts.

7.4 Trace element variation

Only precise trace element data obtained by ICP-MS (Lee et al., 2012 and this study) are used for this discussion. The Ellsworth-Whitmore terrane granites as a whole have coherent trace element variations. There is a strong overall correlation between Ca and Sr (Fig. 8a), consistent with plagioclase fractionation reducing Ca and Sr in more evolved magmas. Sr is therefore used as an approximate (inverse) index of fractionation. The Nash Hills samples are the least fractionated in Fig. 8a; this is partly a result of sample selection as more fractionated granites exist from this intrusion (Fig. 6). The very low Sr abundances of the Pirrit Hills granite are consistent with a relatively high degree of fractionation of this granite. The positive correlation of Zr with Sr (Fig. 8b) indicates progressive removal of Zr during magma evolution probably as a result of fractional removal of zircon. The plot of Eu/Eu^* (Eu^* is Eu predicted from Sm and Gd abundances) versus Sr (Fig. 8c) shows a similar relationship to Zr versus Sr. This suggests removal of Eu during progressive fractional crystallisation of plagioclase. The distribution for La_N/Yb_N (chondrite normalised La/Yb) is similar to those for Zr and Eu/Eu^* (Fig. 8d). During the fractionation interval represented by the samples, compositions evolved from LREE-enriched (La_N/Yb_N in the range 6.7-13.6 in Pagano, Linck and Nash granites) to significantly LREE-depleted ($\text{La}_N/\text{Yb}_N < 0.5$ in the more evolved Pirrit Hills samples). The distribution is interpreted to result from removal of light rare earth elements (LREE) such as La in preference to heavy rare earth elements (HREE) such as Yb in a fractionating phase. As neither La nor Yb is likely to have been fractionally removed by any of the observed phenocryst phases, it is likely that a minor LREE-bearing mineral such as allanite was part of the fractionating assemblage.

Th and U have a different relationship to the fractionation index, Sr (Fig. 8e, f). There is no systematic overall trend in abundances of either element with Sr. This suggests that, during fractional crystallisation, removal of Th and U in any minor phases was in approximate balance with increase in abundances in the liquid. The overall ranges in the granite group are 8.1-51.9 ppm for Th (60.7 ppm in altered Martin Hills sample R.2230.7) and 4.0-28.6 ppm for U. These important heat producing elements are discussed further below, but we note here that the

granites overwhelmingly have significantly higher Th and U abundances than those of average upper continental crust (Th, 10.5 ppm; U, 2.7 ppm; Rudnick and Gao, 2003).

Chondrite-normalised multi-element plots (Fig. 9) for samples from all four granites show a general relative enrichment in more incompatible elements in mantle on the left of the diagram compared to less incompatible elements on the right, consistent with both derivation from incompatible element-enriched mafic magma and by melting of continental crust. The depletions in Nb relative to other elements of similar incompatibility are also consistent with derivation from Nb-depleted continental basalt or continental crust. The samples have variably pronounced depletions in Ba, K, Sr and Zr relative to other trace elements of similar incompatibility in mantle, consistent with removal of alkali feldspar, plagioclase and zircon during fractionation. In Fig. 9a, altered Martin Hills sample R.2230.7 is compared to a Nash Hills sample from the same intrusion. The Martin Hills sample is relatively depleted in Ba, K and Rb, probably as a result of the alteration. The Pagano Nunatak and Linck Nunataks samples (Fig. 9b) have similar abundances to those of the Nash Hills granite, although less enriched in rare earth elements (REE). The Pirrit Hills granite samples (Fig. 8c) have flatter patterns in the REE, a result of the LREE depletion discussed above, and very low Ba and Sr abundances resulting from feldspar fractionation. Fig. 9 also compares the granites to calculated average upper continental crust (Rudnick and Gao, 2003). The granite patterns are generally similar to that of the crust composition, although more depleted in Sr and Zr which is an indication of the relatively extreme fractionation of the granites. Significantly, the granites have higher Th, U and K abundances than the average upper crust.

7.5 Heat Production

Heat production is the heat generated in rocks by radioactive decay. Some 98% of heat production in crustal rocks is from the elements K, U and Th (Beardsmore and Cull, 2001). A calculation of the heat production of the Jurassic Ellsworth-Whitmore terrane granites following the methods of Beardsmore and Cull (2001) is shown in Table 3 with further explanation in Supplementary Material. Most of the heat production is generated by U and Th

with K generating only 3.4-15.4% of the totals. In Fig. 10, calculated heat production is plotted against whole rock U and Th abundances of the granites. The overall variations in both U and Th in these granites as depicted in the figure are not related in a simple way to fractional crystallization, as there is little variation in abundances of either element with Sr values (Fig. 8). The Jurassic granites have heat production values ranging from $2.96 \mu\text{W}/\text{m}^3$ in a Linck Nunatak sample to $9.06 \mu\text{W}/\text{m}^3$ in a Nash Hills sample. The mean value for the Jurassic Ellsworth-Whitmore terrane granites is $5.35 \mu\text{W}/\text{m}^3$. These values are significantly higher than the heat production of $1.65 \mu\text{W}/\text{m}^3$ for calculated average upper continental crust (Fig. 10). Incomplete data of Vennum and Storey (1987) suggest that the Mount Seelig granite also has high heat production.

Fig. 10 also shows heat production values and U and Th abundances for two further sets of silicic rocks. The Mapple Formation samples are rhyolitic ignimbrites emplaced in the eastern Antarctic Peninsula (Fig. 1) during the eruption of the Chon Aike silicic large igneous province that is related to the eruption of the Karoo-Ferrar flood basalts, extension in the Weddell rift and the onset of Gondwana break-up (Pankhurst et al., 1998; Riley et al., 2001). They are modelled to have been generated by partial melting of hydrated Proterozoic and younger mafic and silicic continental crust along the West Antarctic active margin (Riley et al., 2001), and are interpreted to be part of the same voluminous outburst of silicic magmatism as the Ellsworth-Whitmore terrane granites (Dalziel et al., 2013). Their calculated heat production values straddle that of average upper continental crust, extending up to $2.46 \mu\text{W}/\text{m}^3$, lower than the lowest value for the approximately contemporaneous Ellsworth-Whitmore terrane granites. Interestingly, despite being part of the same silicic magmatic event, in adjacent terranes within West Antarctica, and underlain by similar Grenvillian (ca. 1100 Ma) basement, they have very different U-Th-heat production systematics.

The other granite data set shown in Fig. 10 is for the Cornubian batholith in southwest England; Vennum and Storey (1987) previously described similarities between this granite batholith and the Ellsworth-Whitmore terrane granites. The Cornubian batholith is a compound granite composed of several granitic intrusions that is post-tectonic in relation to the end-Carboniferous Variscan orogeny and is associated with extension. It is a peraluminous, has a

two-mica mineralogy and is associated with very high heat flow ($>110 \text{ mW/m}^2$) (Stone and Exley, 1985; Webb et al., 1985; Lee et al., 1987). The heat production values of five component intrusions of the Cornubian batholith are similar to those of the Ellsworth-Whitmore terrane granites (Fig. 10).

The South Australia heat flow anomaly (SAHFA), situated along the eastern margin of the Gawler craton and the western margin of the Adelaide fold belt is another province that has high heat flow (mean $92 \pm 10 \text{ mW/m}^2$) associated with granitic magmatism (Neumann et al., 2000). The high heat flow anomaly coincides with Proterozoic granites and volcanics which contain anomalously high U, Th and K, similar to those of the Ellsworth-Whitmore terrane granites but extending to even higher abundances. Heat production of granites associated with the SAHFA ranges from 4.5 to extreme values up to $65 \mu\text{W/m}^3$. Many of the high heat production granites of the province, notably within the eastern Gawler craton have similar U, Th and heat production values to those of the Ellsworth-Whitmore terrane granites.

We identify the Ellsworth-Whitmore terrane granites as high heat production (HHP) granites in view of their heat production values being similar to those of the well-studied high heat production Cornubian and South Australian granites, and much higher than that of average upper continental crust.

7.6 Heat Flow

Estimates can be made of the heat flow anomalies generated by the granitic bodies above that of the regional value. In Fig. 11a, the elevation of heat flow above regional values as a result of the presence of the Ellsworth-Whitmore terrane granites is explored for different effective granite thicknesses. Regional heat flow is a total of heat flow from the mantle, and lower and upper crust layers considered as vertical flow (vector A in Fig. 11b). The heat flow anomaly over a granite intruded into the uppermost crust will be the regional heat flow plus additional heat flow generated by the granite in excess of the upper crust it replaces (vector B in Fig. 11b). The heat flow generated by the granite layer in mW/m^2 is the heat production value in $\mu\text{W/m}^3$ times the thickness of the layer in km (Beardsmore and Cull, 2001). The heat production of the

metasediments replaced by the granite layer can be assumed to be the average upper continental crustal value of $1.65 \mu\text{W}/\text{m}^3$. This is within the range of ca. 1.0-1.9 for rift-related sandstone-mudstone sedimentary sequences (Jaupart and Mareschal, 2011). If these assumptions are correct, the excess heat production of the granite layer with the mean heat production value of $5.35 \mu\text{W}/\text{m}^3$ is $3.7 \mu\text{W}/\text{m}^3$ above that of the replaced metasediments.

Because the granites have finite radiuses, their localised heat flow anomalies will be reduced by horizontal heat transfer, although the heat will be retained regionally; the calculations of Jaupart (1983) suggest a local heat flow anomaly reduction by ca. 70% for a granite thickness of 8 km and radius of 20 km.

Modelling of aerogravity and aeromagnetic data (Fig. 4) has suggested a thickness of up to 8 km for the Nash Hills granite and up to 9 km for the Pagano Nunatak granite (Jordan et al., 2013). A significant unknown parameter is the vertical distribution of heat production elements within the granites as a result of the fractionation evolution of the granitic magmas. If the surface heat flow value were known, vertical heat production variations could be assessed. Lee et al. (1987) and Webb et al. (1987) contrasted two UK granite batholiths in the Eastern Highlands of Scotland and SW England. The batholiths have similar, high surface heat production values, but SW England has higher heat flow. They concluded that that heat producing elements reduce in abundance rapidly with depth in the Scottish granites but are present at approximately their measured surface values to a depth of some 15 km in the SW England case. The approximately constant Th and U abundances of the Ellsworth-Whitmore terrane granites when plotted against fractionation indices (Fig. 8 e, f) suggests that heat production similarly may not reduce rapidly with depth.

Estimates of regional heat flow in the Ellsworth-Whitmore terrane and the adjacent Weddell Sea rift system suggest values of $55\text{-}65 \text{ mW}/\text{m}^2$ (Ramirez et al., 2016), consistent with interpretations of satellite magnetic data (Fox-Maule et al., 2005) and seismic data (Shapiro and Ritzwoller, 2004; An et al., 2015a). For this range of regional heat flow values, a 8 km thick granite with uniform heat production produces heat flow over the granite of 84.6 to $94.6 \text{ mW}/\text{m}^2$ (Fig. 11a) which may be realistic for the Pagano and Nash Hills intrusions. A 4 km thick granitic high heat production layer would produce localised heat flow of 69.8 to $79.8 \text{ mW}/\text{m}^2$

for the same regional heat flow values (Fig. 11a). These values may approximate those of thinner granite intrusions, or thicker intrusions in which abundances heat producing elements decline with depth. The modelled heat flow values of 70-95 mW/m² are among the highest predicted values in Antarctica away from direct sources of volcanic/geothermal heat.

7.6 Glaciological implications

It is not possible to demonstrate direct causative links between the modelled heat flow anomalies and glaciological processes with available data. Nevertheless, there are indications of basal melting of ice sheets near the granites both in the present and geological past. Four subglacial lakes occur downstream to the north and east of the granites (Fig. 3a). The granites are situated near the onset of enhanced glacial flow in the Möller and Institute ice streams, and the Siple Coast ice streams (Fig. 2a). A zone in which ancient subglacial meltwater channels have been identified is situated west of the geophysically-identified subcrop of the Pagano Nunatak granite (Rose et al., 2014; Fig. 2a). These meltwater channels are interpreted to have formed during the warmer Pliocene period under temperate ice sheet conditions. None of these indicate subglacial melting directly over the granites. However, the indications of possible warm basal conditions indicate that the granites warrant further investigation as sources of subglacial heat.

8. Source of the enrichment in heat producing elements

As is the case in other high heat production granites (Exley and Stone, 1985), the heat producing elements in the Ellsworth-Whitmore terrane granites are likely to have originated in pelitic metasediments or in Th-U enriched mantle-derived magmas. The origin of the enrichment in U beneath the Weddell rift is explored in Fig. 12. The figure plots the ²⁰⁶Pb/²³⁸U age of zircon grains separated from the granites against the U abundances determined on the same analysis spots. Inherited zircons extend back in age to 1042 Ma, close to the Middle Proterozoic (Grenvillian) thought, from isotope model ages, to be the time of formation of most West Antarctic crust (Millar and Pankhurst, 1987; Pankhurst et al., 1991; Millar et al., 2001;

Flowerdew et al., 2006). All the observed inherited grains older than 300 Ma have U abundances of <2000 ppm, and in most cases <1000 ppm. The Jurassic granites have a much larger range in zircon U abundances. Most of the Jurassic zircons have U abundances <2000 ppm, similar to the inherited zircons, but a significant minority have high U abundances extending to > 13000 ppm. The high U abundances in zircons are observed in data from all of the Linck Nunataks, Pagano Nunataks and Pirrit Hills granites, and in the data sets of both Lee et al. (2012) and Craddock et al. (2017).

As U abundances in zircons can be assumed to be governed by liquid-crystal distribution coefficients, and that limited or no diffusion of U has taken place, it is reasonable to assume that the Jurassic zircons grew in equilibrium with at least two end-member magma compositions: the first had zircons with low U contents similar to the inherited zircons, whilst the second was significantly more U-enriched. The U-enriched zircons of the Ellsworth-Whitmore granite are not unique within West Antarctica, as zircons with >2000 ppm U, all with Mesozoic ages, have been observed in a Jurassic tuff from Thurston Island (Riley et al 2017b), and Jurassic and Cretaceous granites from the Antarctic Peninsula (Riley et al., 2017a; Riley et al., submitted). However, zircons with >2000 ppm U form just 1-5% of the total zircon population in Thurston Island and the Antarctic Peninsula examples which contrasts with 24% in the Jurassic Ellsworth-Whitmore granites, in which the U zircon abundances also extend to higher values. Our interpretation is that significant amounts of high-U liquid became available in the source areas of the Jurassic granites of the Ellsworth-Whitmore terrane by the time that the granitic magmas formed, and that such a high-U source was not previously present regionally in significant volumes.

Examination of Fig. 12 indicates that the influx of the high-U source started before Jurassic times. One zircon in the 200 Ma Mount Seelig granite has a U abundance of 5618 and an age of 200.3 ± 2.1 Ma, a similar age to the low-U zircons in the same granite, suggesting that the high-U source was present in the crust by that time. The Linck Nunataks granite contains four zircons with over 2300 ppm U and with ages of 217-299 Ma (Craddock et al., 2017). As zircon grains with high U contents are likely to yield erroneously old SIMS ages (White and Ireland, 2012) these ages should be treated with caution. It is likely that the two grains with the highest U

contents have erroneous ages U-Pb ages resulting from the high-U matrix effect. However, the two grains with U abundances of 4717 and 2331 ppm and $^{206}\text{Pb}/^{238}\text{U}$ ages of 299 and 244 Ma respectively are less plausibly erroneous due to this effect and are significant older than trends resulting from the high-U matrix effect depicted for zircons in similar age Ferrar basalts by White and Ireland (2012). We suggest that these data indicate that the high-U source was first present beneath the Ellsworth-Whitmore terrane by at least the age of the Mount Seelig granite which, at 200 Ma, significantly pre-dated the initiation of Gondwana break-up and eruption of the Karoo and Ferrar large igneous province at ca. 182-183 Ma (Svensen et al., 2012, Burgess et al., 2015). The high-U source may have been present by ca. 299 Ma. There is no indication from the inherited zircons that it appeared before that time, indicating that Grenvillian basement was not the source. The process of U-enrichment of the source may have continued into Jurassic times in association with rifting and magmatism related to Gondwana break-up, but this would have been a continuation of previous events. The significant geological event in this part of Antarctica during the period between 299 and 200 Ma was the formation of the late Palaeozoic – early Mesozoic Gondwanide fold belt (Dalziel et al., 2013). This was a compressional fold belt that trended parallel to, but inboard of, the Gondwana-Pacific margin and extended from Sierra de la Ventana in Argentina through the Cape Fold Belt in South Africa to the Pensacola Mountains along the East Antarctic margin of Antarctica and was dispersed during Gondwana break-up (Fig. 2b). Its major compressive phase is Ar-Ar dated to 275-260 Ma in the Cape Fold Belt (Hansma et al., 2016). It was this major tectonic event that deformed the sedimentary sequence of the Ellsworth Mountains (Curtis, 2001). This orogeny may have resulted in transfer of high-U material to the lower-mid crust of the Ellsworth-Whitmore terrane as fertile metasediments during over-thrusting, lateral escape or post-orogenic extension involving low-angle faults. An alternative mechanism would be by intrusion of high-U mantle derived magmas into the lower-mid crust either during orogenesis or during post-orogenic extension, as observed in the late- and post-orogenic stages of many orogens (e.g. European Variscan, von Seckendorff et al., 2004; Himalaya, Miller et al., 1999). Low extension and magma flux rates during post-orogenic extension are more likely to generate relatively small-volume, potassic, high-U magmas than the high extension and magma flux rates

associated with the Jurassic rifting and break-up events. Partial melting of a low-mid crustal source enriched in U, Th and K via heating during Jurassic magmatism is the most plausible source for the Jurassic high-heat production granites.

9. Conclusions

1. The four known Jurassic Ellsworth-Whitmore granites, exposed at Pagano Nunatak, Pirrit Hills, Nash-Martin Hills and Linck Nunataks were emplaced during extension and transtension within the adjacent Weddell Sea continental rift system. The Pagano Nunatak granite was emplaced within the transtensional Pagano shear zone.
2. A new zircon U-Pb ion-microprobe age of 178.0 ± 3.5 Ma for the Pirrit Hills granite, is interpreted as the age of emplacement. The precise U-Pb ages of 178-174 Ma for the Ellsworth-Whitmore terrane granites significantly post-date the ages of eruption of the Ferrar and Karoo Basin basalts, and these basalts could not have provided the heat source for crustal melting to form the granites. However, the ages of the granites fall within the more extended age range of the Chon Aike silicic LIP.
3. The granites are mildly peraluminous, two-mica granites that are classified as A-type (within-plate), and have some S-type characteristics. They have similar alkali elements and aluminium saturation characteristics to many Triassic-Cretaceous granitoids in the adjacent Antarctic Peninsula.
4. Because of their high K and especially U and Th contents, these intrusions are high heat production (HHP) granites, with heat production in the range $2.96 \mu\text{W}/\text{m}^3$ in a Linck Nunatak sample to $9.06 \mu\text{W}/\text{m}^3$ in a Nash Hills sample. The mean value for the Jurassic Ellsworth-Whitmore terrane granites is $5.35 \mu\text{W}/\text{m}^3$, significantly higher than the upper continental crust average.
5. Such high heat production is expected to result in local heat flow anomalies of 15-30 mW/m^2 above the regional value for the rift. Total heat flow above the granite

intrusions is predicted to be in the range 70-95 mW/m² depending on the thickness of the high heat production granite layer and the regional heat flow value.

6. Investigation of U abundances and U-Pb ages of separated detrital and Jurassic zircons reveals that the high-U source equated with origin of the high heat producing elements was introduced beneath the Weddell rift by 299-200 Ma, before the initiation of Gondwana break-up. There is no evidence from the zircons that it was present before 299 Ma. The introduction of the high-U source may have coincided with the deformation and post-orogenic extension of the Gondwanide fold belt.

Acknowledgements

This study is part of the British Antarctic Survey Polar Science for Planet Earth Programme and was partly funded by the Natural Environment Research Council (UK). Samples can be accessed at the British Antarctic Survey, Cambridge. This is NORDSIM publication number [number to be assigned]. The NORDSIM facility is operated under an agreement between the research funding agencies of Denmark, Norway and Sweden, the Geological Survey of Finland and the Swedish Museum of Natural History.

References

- An, M., Wiens, D.A., Zhao, Y., Feng, M., Nyblade, A., Kanao, M., Li, Y., Maggi, A., L  v  que, J.-J., 2015a. Temperature, lithosphere-asthenosphere boundary, and heat flux beneath the Antarctic plate inferred from seismic velocities. *Journal of Geophysical Research Solid Earth* 120, 8720-8742, doi: 10.1002/2015JB011917.
- An, M., Wiens, D.A., Zhao, Y., Feng, M., Nyblade, A., Kanao, M., Li, Y., Maggi, A., L  v  que, J.-J., 2015b. S-velocity model and inferred Moho topography beneath the Antarctic plate from Rayleigh waves. *Journal of Geophysical Research Solid Earth* 120, 359-383, doi: 10.1002/2014JB011332.

- Beardsmore, G.R., Cull, J.P., 2001. *Crustal Heat Flow: A Guide to Measurement and Modelling*. Cambridge University Press, Cambridge, 324 pp.
- Bingham, R.G., Siegert, M.J., 2007. Radar-derived bed roughness characterization of Institute and Möller ice streams, West Antarctica, and comparison with Siple Coast ice streams. *Geophysical Research Letters* 34, L21504, doi:10.1029/2007GL031483.
- Block, A.E., Bell, R.E., Studinger, M., 2009. Antarctic crustal thicknesses from satellite gravity: implications for the Transantarctic Mountains and Gamburtsev Subglacial Mountains. *Earth and Planetary Science Letters* 288, 194-203.
- Burgess, S.D., Bowring, S.A., Fleming, T.H., Elliot, D.H., 2015. High-precision geochronology links the Ferrar large igneous province with early-Jurassic ocean anoxia and biotic crisis. *Earth and Planetary Science Letters* 415, 90-99.
- Burton-Johnson, A., Halpin, J.A., Whittaker, J.M., Graham, F.S., Watson, S.J., 2017. A new heat flux model for the Antarctic Peninsula incorporating spatially variable upper crustal radiogenic heat production. *Geophysical Research Letters* 44, 10.1002/2017GL073596.
- Carson, C.J., McLaren, S., Roberts, J.L., Boger, S.D., Blankenship, D.D., 2014. Hot rocks in a cold place: high sub-glacial heat flow in East Antarctica. *Journal of the Geological Society, London* 171, 9-12.
- Charoy, B., 1986. The Genesis of the Cornubian Batholith (South-West England): the example of the Carnmenellis Pluton. *Journal of Petrology* 27, 571-604.
- Craddock, J.P., Schmitz, M.D, Crowley, J.L., Larocque, J., Pankhurst, R.J., Juda, N., Konstantinou, A., Storey, B., 2017. Precise U-Pb zircon ages and geochemistry of Jurassic granites, Ellsworth-Whitmore terrane, central Antarctica. *Geological Society of America Bulletin* 129, 118-136.
- Curtis, M.L., 2001. Tectonic history of the Ellsworth Mountains, West Antarctica: Reconciling a Gondwana enigma. *Geological Society of America Bulletin* 113, 939-958.
- Curtis, M.L., Storey, B.C., 1996. A review of geological constraints on the pre-break-up position of the Ellsworth Mountains within Gondwana: implications for Weddell Sea evolution, in:

- Storey, B.C., King, E.C., Livermore, R.A. (Eds.), Weddell Sea Tectonics and Gondwana Break-up. Geological Society, London, Special Publications 108, 11-30.
- Curtis, M.L., Leat, P.T., Riley, T.R., Storey, B.C., Millar, I.L., Randall, D.E., 1999. Middle Cambrian rift-related volcanism in the Ellsworth Mountains, Antarctica: tectonic implications for the palaeo-Pacific margin of Gondwana. *Tectonophysics* 304, 275-299.
- Dalziel, I.W.D., 1991. Pacific margins of Laurentia and East Antarctica-Australia as a conjugate rift pair: evidence and implications for an Eocambrian super continent. *Geology* 19, 598-601.
- Dalziel, I.W.D., Lawver, L.A., Norton, I.O., Gahagan, L.M., 2013. The Scotia arc: genesis, evolution, global significance. *Annual Review of Earth and Planetary Sciences* 41, 767-693.
- Elliot, D.H., Fleming, T.H., 2004. Occurrence and dispersal of magmas in the Jurassic Ferrar large igneous province, Antarctica. *Gondwana Research* 7, 223-237.
- Ferraccioli, F., Jones, P.C., Vaughan, A.P.M., Leat, P.T., 2006. New aerogeophysical view of the Antarctic Peninsula: more pieces, less puzzle. *Geophysical Research Letters* 33, L05310, 10.1029/2005GL024636.
- Fleming, T.H., Heimann, A., Foland, K.A., Elliot, D.H., 1997. $^{40}\text{Ar}/^{39}\text{Ar}$ geochronology of Ferrar dolerite sills from the Transantarctic Mountains, Antarctica: implications for the age and origin of the Ferrar magmatic province. *Geological Society of America Bulletin* 109, 533-546.
- Flowerdew, M.J., Millar, I.L., Curtis, M.L., Vaughan, A.P.M., Horstwood, M.S.A., Whitehouse, M.J., Fanning, C.M., 2007. Combined U-Pb geochronology and Hf isotope geochemistry of detrital zircons from early Paleozoic sedimentary rocks Ellsworth-Whitmore mountains block, Antarctica. *Geological Society of America Bulletin* 119, 275-288.
- Flowerdew, M.J., Millar, I.L., Vaughan, A.P.M., Horstwood, M.S.A., Fanning, C.M., 2006. The source of granitic gneisses and migmatites in the Antarctic Peninsula: a combined U-Pb SHRIMP and laser ablation Hf isotope study of complex zircons. *Contributions to Mineralogy and Petrology* 151, 751-768.
- Fox Maule, C., Purucker, M.E., Olsen, N., Mosegaard, K., 2005. Heat flux anomalies in Antarctica revealed by satellite magnetic data. *Science* 309, 464-467. 10.1126/science.1106888.

- Garrett, S.W., Maslanyj, M.P., Damaske, D., 1988. Interpretation of aeromagnetic data from the Ellsworth Mountains-Theil Mountains ridge, West Antarctica. *Journal of the Geological Society, London* 145, 1009-1017.
- Grunow, A.M., Kent, D.V., Dalziel, I.W.D., 1987. Mesozoic evolution of West Antarctica and the Weddell Sea basin: new paleomagnetic constraints. *Earth and Planetary Science Letters* 86, 16-26.
- Haapala, I., 1997. Magmatic and postmagmatic processes in tin-mineralized granites: topaz-bearing leucogranite in the Eurajoki Rapakivi granite stock, Finland. *Journal of Petrology* 38, 1645-1659.
- Hansma, J., Tohver, E., Schrank, C., Jourdan, F., Adams, D., 2016. The timing of the Cape Orogen: new $^{40}\text{Ar}/^{39}\text{Ar}$ age constraints on deformation and cooling of the Cape Fold Belt, South Africa. *Gondwana Research* 32, 122-137.
- Jordan, T. A., Ferraccioli, F., Ross, N., Siegert, M.J., Corr. H.F., Leat, P.T., Bingham, R.G., Rippin, D.M., 2013. Structure and inland extent of the Mesozoic Weddell Sea Rift, Antarctica, imaged by new aerogeophysical data. *Tectonophysics* 585, 137-160.
- Jordan, T.A., Ferraccioli, F., Leat, P.T., 2017. A new model for microplate movement, magmatism, and distributed extension in the Weddell Sea Rift System of West Antarctica. *Gondwana Research* 42, 29-48.
- Jaupart, C., 1983. Horizontal heat transfer due to radioactivity contrasts: causes and consequences of the linear heat flow relation. *Geophysical Journal of the Royal Astronomical Society* 75, 411-435.
- Jaupart, C., Mareschal, J.-C., 2011. *Heat Generation and Transport in the Earth*. Cambridge University Press, Cambridge. 477pp.
- King, E.C., 2000. The crustal structure and sedimentation of the Weddell Sea embayment: implications for Gondwana reconstructions. *Tectonophysics* 327, 195-212.

- King, E.C., Bell, A.C., 1996. New seismic data from the Ronne Ice Shelf, Antarctica, in: Storey, B.C., King, E.C., Livermore, R.A. (Eds.), *Weddell Sea Tectonics and Gondwana Break-up*. Geological Society, London, Special Publications 108, 213-226.
- King, E.C., Livermore, R.A., Storey, B.C., 1996. Weddell Sea tectonics and Gondwana break-up: an introduction, in: Storey, B.C., King, E.C., Livermore, R.A. (Eds.), *Weddell Sea Tectonics and Gondwana Break-up*. Geological Society, London, Special Publications 108, 1-10.
- Leat, P.T., Scarrow, J.H., Millar, I.L., 1995. On the Antarctic Peninsula batholith. *Geological Magazine* 132, 399-4127.
- Leat, P.T., Scarrow, J.H., Wareham, C.D., 1997. A model for Late Triassic to Early Cretaceous Antarctic Peninsula Plutonism, in: Ricci, C.A. (Ed.), *The Antarctic Region: Geological Evolution and Processes*. Terra Antarctica Publications, Siena, pp. 321-326.
- Leat, P.T., Dean, A.A., Millar, I.L., Kelley, S.P., Vaughan, A.P.M., Riley, T.R., 2005. Lithospheric mantle domains beneath Antarctica, in: Vaughan, A.P.M., Leat, P.T., Pankhurst, R.J. (Eds.), *Terrane Processes at the Margins of Gondwana*. Geological Society, London, Special Publications 246, 359-380.
- Lee, D.E., Kistler, R.W., Friedman, I., Van Loenen, R.E., 1981. Two-mica granites of northeastern Nevada. *Journal of Geophysical Research* 86, 10607-10616.
- Lee, H.M., Lee, J.I., Lee, M.J., Kim, J., Choi, S.W., 2012. The A-type Pirrit Hills Granite, West Antarctica: an example of magmatism associated with the Mesozoic break-up of the Gondwana supercontinent. *Geosciences Journal* 16, 421-433.
- Lee, M.K., Brown, G.C., Webb, P.C., Wheildon, J., Rollin, K.E., 1987. Heat flow, heat production and thermo-tectonic setting in mainland UK. *Journal of the Geological Society, London* 144, 35-42.
- Leitchenkov, G.L., Kudryavtzev, G.A., 1997. Structure and origin of the Earth's Crust in the Weddell Sea Embayment (beneath the front of the Filchner and Ronne ice shelves) from deep seismic sounding data. *Polarforschung* 67, 143-154

- Llubes, M., Lansaeu, C., Rémy, F., 2006. Relations between basal condition, subglacial hydrological networks and geothermal flux in Antarctica. *Earth and Planetary Science Letters* 241, 655-662.
- Manning, D.A.C., Exley, C.S., 1984. The origins of late-stage rocks in the St Austell Granite – a re-interpretation. *Journal of the Geological Society, London* 141, 581-591.
- Millar, I.L., Pankhurst, R.J., 1987. Rb-Sr geochronology of the region between the Antarctic Peninsula and the Transantarctic mountains: Haag Nunataks and Mesozoic granitoids, in: McKenzie, G.D. (Ed.), *Gondwana Six: Structure, Tectonics and Geophysics*. American Geophysical Union Geophysical Monographs 40, 151-160.
- Millar, I.L., Willan, R.C.R., Wareham, C.D., Boyce, A.J., 2001. The role of crustal and mantle sources in the genesis of granitoids of the Antarctic Peninsula and adjacent crustal blocks. *Journal of the Geological Society, London* 158, 855-867.
- Miller, C., Schuster, R., Klötzli, U., Frank, W., Purtscheller, F., 1999. Post-collisional potassic and ultrapotassic magmatism in SW Tibet: geochemical and Sr-Nd-Pb-O isotopic constraints for mantle source characteristics and petrogenesis. *Journal of Petrology* 40, 1399-1424.
- Morin, R.H., Williams, T., Henrys, S.A., Mogens, D., Niessen, F., Hansaraj, D., 2010. Heat flow and hydrologic characteristics at the AND-1B borehole, ANDRILL McMurdo Ice Shelf Project, Antarctica. *Geosphere* 6, 370-378.
- Neumann, N., Sandiford, M., Foden, J., 2000. Regional geochemistry and continental heat flow: implications for the origin of the South Australian heat flow anomaly. *Earth and Planetary Letters* 183, 107-120.
- Pankhurst, R.J., Storey, B.C., Millar, I.L., 1991. Magmatism related to the break-up of Gondwana, in: Thomson, M.R.A., Crame, J.A., Thomson, J.W. (Eds.), *Geological Evolution of Antarctica*. Cambridge University Press, Cambridge, pp. 573-579.
- Pankhurst, R.J., Leat, P.T., Sruoga, P., Rapela, C.W., Márquez, M. Storey, B.C., Riley, T.R., 1998. The Chon Aike silicic province of Patagonia and related rocks in West Antarctica: a silicic large igneous province. *Journal of Volcanology and Geothermal Research* 81, 113-136.

- Pankhurst, R.J., Riley, T.R., Fanning, C.M., Kelley, S.P., 2000. Episodic silicic magmatism in Patagonia and the Antarctic Peninsula: chronology of magmatism associated with the break-up of Gondwana. *Journal of Petrology* 41, 605-625.
- Payne, A.J., 1998. Dynamics of the Siple Coast ice streams, West Antarctica: results from a thermomechanical ice sheet model. *Geophysical Research Letters* 25, 3173-3176.
- Pollard, D., DeConto, R. M., 2003, Antarctic ice and sediment flux in the Oligocene simulated by a climate-ice sheet-sediment model. *Palaeogeography, Palaeoclimatology, Palaeoecology* 198, 53-67.
- Pollard, D., DeConto, R.M., Nyblade, A.A., 2005. Sensitivity of Cenozoic Antarctic ice sheet variations to geothermal heat flux. *Global and Planetary Change* 49, 63-74.
- Ramirez, C., Nyblade, A., Hansen, S.E., Wiens, D.A., Anandakrishnan, S., Aster, R.C., Huerta, A.D., Shore, P., Wilson, T., 2016. Crustal and upper-mantle structure beneath ice-covered regions in Antarctica from S-wave receiver functions and implications for heat flow. *Geophysical Journal International* 204, 1636-1648.
- Randall, D.E., Mac Niocaill, C., 2004. Cambrian palaeomagnetic data confirm a Natal Embayment location for the Ellsworth–Whitmore Mountains, Antarctica, in Gondwana reconstructions. *Geophysical Journal International* 157, 105-116.
- Riley, T.R., Burton-Johnson, A., Flowerdew, M.J., Whitehouse, M.J., submitted. Episodicity within a mid-Cretaceous magmatic flare-up in West Antarctica: U-Pb ages of the Lassiter Coast intrusive suite, Antarctic Peninsula and correlations along the Gondwana margin. *Geological Society of America Bulletin*.
- Riley, T.R., Flowerdew, M.J., Pankhurst R.J., Curtis, M.L, Millar, I.L., Fanning, C.M., Whitehouse, M.J., 2017a. Early Jurassic magmatism on the Antarctic Peninsula and potential correlation with the Subcordilleran plutonic belt of Patagonia. *Journal of the Geological Society, London* 174, 365-376.

- Riley, T.R., Flowerdew, M.J., Pankhurst, R.J., Leat, P.T., Millar, I.L., Fanning, C.M., Whitehouse, M.J., 2017b. A revised geochronology of Thurston Island, West Antarctica, and correlations along the proto-Pacific margin of Gondwana. *Antarctic Science* 29, 47-60.
- Riley, T.R., Leat, P.T., Pankhurst, R.J., Harris, C., 2001. Origins of large volume rhyolitic volcanism in the Antarctic Peninsula and Patagonia by crustal melting. *Journal of Petrology* 42, 1043-1065.
- Rignot, E., Mouginot, J., Scheucht, B., 2011. Ice flow of the Antarctic ice sheet. *Science* 333, 1427-1430.
- Ritzwoller, M.H., Shapiro, N.M., Levshin, A.L., Leahy, G.M., 2001. Crustal and upper mantle structure beneath Antarctica and surrounding oceans. *Journal of Geophysical Research* 106, 30645-30670.
- Rose, K.C., Ross, N., Bingham, R.G., Corr, H.F.J., Ferraccioli, F., Jordan, T.A., Le Brocq, A.M., Rippin, D.M., Siegert, M.J., 2014. A temperate former West Antarctic ice sheet suggested by an extensive zone of subglacial meltwater channels. *Geology* 42, 971-974.
- Rudnick, R.L., Gao, S., 2003. Composition of the Continental Crust, in: Rudnick, R.L. (Ed.), *The Crust, Treatise on Geochemistry, Volume 3*, Elsevier, pp 1-64.
- Scarrow, J.H., Pankhurst, R.J., Leat, P.T., Vaughan, A.P.M., 1996. Antarctic Peninsula granitoid petrogenesis: a case study from Mount Charity, north-eastern Palmer Land. *Antarctic Science* 8, 193-206.
- Shapiro, N.M., Ritzwoller, M.H., 2004. Inferring surface heat flow distributions guided by a global seismic model: particular application to Antarctica. *Earth and Planetary Science Letters* 223, 213-224.
- Schroeder, D.M., Blankenship, D.D., Young, D.A., Quartini, E., 2014. Evidence for elevated and spatially variable geothermal flux beneath the West Antarctic Ice Sheet. *Proceedings of the National Academy of Science of the United States of America* 111, 9070-9072.

- Siegert, M.J., Ross, N., Corr, H., Smith, B., Jordan, T., Bingham, R.G., Ferraccioli, F., Rippin, D.M., Le Brocq, A., 2014. Boundary conditions of an active West Antarctic subglacial lake: implications for storage of water beneath the ice sheet. *The Cryosphere* 8, 15-24.
- Smith, B.E., Fricker, H.A., Joughin, I.R., Tulaczyk, S., 2009. An inventory of active subglacial lakes in Antarctica detected by ICESat (2003-2008). *Journal of Glaciology* 55, 573-595.
- Storey, B.C., Dalziel, I.W.D., 1987. Outline of the structural and tectonic history of the Ellsworth-Whitmore mountains-Thiel Mountains ridge, West Antarctica, in: McKenzie, G.D. (Ed.), *Gondwana Six: Structure, Tectonics and Geophysics*. American Geophysical Union Geophysical Monographs 40, 117-128.
- Storey, B.C., Dalziel, I.W.D., Garrett, S.W., Grunow, A.M., Pankhurst, R.J., Vennum, W.R., 1988a. West Antarctica in Gondwanaland: Crustal blocks, reconstruction and breakup processes. *Tectonophysics* 155, 381-390.
- Storey, B.C., Hole, M.J., Pankhurst, R.J., Millar, I.L., Vennum, W., 1988b. Middle Jurassic within-plate granites in West Antarctica and their bearing on the break-up of Gondwanaland. *Journal of the Geological Society, London* 145, 999-1007.
- Stone, M., Exley, C.S., 1985. High heat production granites of southwest England and their associated mineralization: a review, in: Halls, C. (Ed.), *High Heat Production (HHP) Granites, Hydrothermal Circulation and Ore Genesis*. Institution of Mining and Metallurgy, London, pp. 571-593.
- Studinger, M., Miller, H., 1999. Crustal structure of the Filchner-Ronne shelf and Coasts Land, Antarctica, from gravity and magnetic data: implications for the breakup of Gondwana. *Journal of Geophysical Research* 104, 20379-20394.
- Sun, S.-s., McDonough, W.F., 1989. Chemical and isotopic systematics of oceanic basalts: implications for mantle composition and processes, in: Saunders, A.D., Norry, M.J. (Eds.), *Magmatism in the Ocean Basins*. Geological Society, London, Special Publications 42, 313-345.

- Svensen, H., Corfu, F., Polteau, S., Hammer, O., Planke, S., 2012. Rapid magma emplacement in the Karoo large igneous province. *Earth and Planetary Science Letters* 325-326, 1-9.
- Veevers, J.J., 2012. Reconstructions before rifting and drifting reveal the geological connections between Antarctica and its conjugates within Gondwanaland. *Earth Science Reviews* 111, 249-318.
- Vennum, W.R., Storey, B.C., 1987b. Petrology, geochemistry, and tectonic setting of granitic rocks from the Ellsworth-Whitmore Mountains crustal block and Thiel Mountains, West Antarctica, in: McKenzie G.D. (Ed.), *Gondwana Six: Structure, Tectonics and Geophysics*. American Geophysical Union Geophysical Monographs 40, 139-150.
- Vidal, Ph., Cocherie, A., Le Fort, P., 1982. Geochemical investigations of the origin of the Manaslu leucogranite (Himalaya, Nepal). *Geochimica et Cosmochimica Acta* 46, 2279-2292.
- von Seckendorff, V., Timmerman, M.J., Kramer, W., Wrobel, P., 2004. New $^{40}\text{Ar}/^{39}\text{Ar}$ ages and geochemistry of late Carboniferous-early Permian lamprophyres and related volcanic rocks in the Saxothuringian Zone of the Variscan Orogen (Germany), in: Wilson, M., Neumann, E.-R., Davies, G.R., Timmerman, M.J., Heermans, M., Larsen B.T. (Eds.), *Permo-Carboniferous Magmatism and Rifting in Europe*. Geological Society, London, Special Publications, 223, 335-359.
- Whitehouse, M.J., Kamber, B., 2005. Assigning dates to thin gneissic veins in high-grade metamorphic terranes: a cautionary tale from Akilia, southwest Greenland. *Journal of Petrology* 46, 291-318.
- Webb, P.C., Tindle, A.G., Barritt, S.D., Brown, G.C., Miller, J.F., 1985. Radiothermal granites of the United Kingdom: comparison of fractionation patterns and variation of heat production for selected granites, in: Halls, C. (Ed.), *High Heat Production (HHP) Granites, Hydrothermal Circulation and Ore Genesis*. Institution of Mining and Metallurgy, London, pp. 409-424.
- Webb, P.C., Lee, M.K., Brown, G.C., 1987. Heat flow – heat production relationships in the UK and the vertical distribution of heat production in granite batholiths. *Geophysical Research Letters* 14, 279-282.

- Weber, G.F., Craddock, C., Rogers, M.A., Anderson, J.J., 1982. Geology of the Whitmore Mountains, in: Craddock, C. (Ed.), Antarctic Geoscience. University of Wisconsin Press, Madison, pp. 841-847.
- Weber, G.F., Craddock, C., Rogers, M.A., Anderson, J.J., 1983. Geology of Pagano Nunatak and the Hart Hills, in: Oliver, R.L., James, P.R., Jago, J.B., (Eds.), Antarctic Earth Science. Australian Academy of Science, Canberra, pp. 251-255.
- Weber, G.F., Craddock, C., Splettstoesser, J.F., 1992. Geology of the Ellsworth Mountains, West Antarctica, in: Weber, G.F., Craddock, C., Splettstoesser, J.F. (Eds.), Geology and Palaeontology of the Ellsworth Mountains, West Antarctica. Geological Society of America, Memoirs 170, 1-7.
- Wever, H.E., Storey, B.C., Leat, P., 1995. Peraluminous granites in NE Palmer Land, Antarctic Peninsula: early Mesozoic crustal melting in a magmatic arc. Journal of the Geological Society, London 152, 85-96.
- White, L.T., Ireland, T.R., 2012. High-uranium matrix effect in zircon and its implications for SHRIMP U-Pb age determinations. Chemical Geology 306-307, 78-91.

Figure captions

Fig. 1. Sketch map of topographic elevation above sea level of part of Antarctica showing location of the Ellsworth-Whitmore terrane (EWT). The EWT separates the Weddell Sea rift system (WSRS) from the West Antarctic rift system (WARS), the later extending to the Transantarctic Mountains (TAM). The Antarctic Peninsula (AP) and Thurston Island (TI) are crustal blocks along the Pacific margin of Antarctica. The locations of the Ellsworth-Whitmore terrane granites are indicated in pink, and the pink outline extending from the AP to TI is the extent of the Antarctic Peninsula batholith (Leat et al., 1995) and associated intrusions defined by the Pacific margin magnetic anomaly (Ferraccioli et al., 2006). ANDRILL is the site of well-determined heat flow from boreholes. The black box shows the area in Fig. 2a.

Fig. 2a. Map of sub-ice topography of the Weddell Sea rift system and the Ellsworth-Whitmore terrane, Antarctica. The Ellsworth-Whitmore terrane forms the topographically high ridge from the Ellsworth Mountains to the Whitmore Mountains and Pagano Nunatak and, with Haag Nunataks (HN), is underlain by the Haag-Ellsworth-Whitmore tectonic block (Storey et al., 1988a; Jordan et al., 2017). The Pagano Shear Zone (PSZ), indicated by the yellow line, forms the southeastern extent of both the Weddell Sea rift system and the Ellsworth-Whitmore terrane (Jordan et al., 2017). The Ellsworth-Whitmore terrane is situated between the Weddell Sea rift system and the West Antarctic rift system. Ice divides (dashed white line) separating the Weddell Sea from the Siple Coast and Amundsen Sea catchments follow the topographic ridge formed by the Ellsworth-Whitmore terrane. White arrows indicate fast-flowing ice streams. The Institute and Moller ice streams (IIS and MIS) originate in the Ellsworth-Whitmore Mountains terrane and flow east and north to the Weddell Sea. Ice streams flow in the opposite direction toward the Siple Coast. The diagonal fill indicated the zone ancient subglacial meltwater channels documented by Rose et al. (2014). Filled circles are outcrops of granites of the Ellsworth-Whitmore terrane: PH, Pirrit Hills; MS, Martin Hills; NH, Nash Hills; PN, Pagano Nunatak; LN, Linck Nunataks; MS, Mount Seelig. HN, Haag Nunataks; DI, Dufek Intrusion; PM, Pensacola Mountains; PAT, Patuxent Range; TM, Thiel Mountains. The red box shows the area covered by Fig. 3. 2b. Tectonic reconstruction of Gondwana at the early stage of break-up

modified after Dalziel et al. (2013). The depicted time of 182 Ma is the age of eruption of the Karoo large igneous province and the filled circle shows the approximate extent of the Karoo mantle plume which is interpreted to have facilitated mantle melting and influencing the locations of rifting. The lines meeting in the Weddell Sea area are rift axes showing the order of major rifting as determined from aerogeophysically observed trends in the Weddell Sea rift system (Jordan et al., 2017). Axis 1, rifting in the southern province of the Weddell Sea rift system; axis 2, rifting in the northern province of the Weddell Sea rift system; axis 3, extension between Pacific margin blocks and the continental interior. The Gondwanide fold belt indicated by blue fill in South America (Sierra de la Ventana), South Africa (Cape Fold Belt), Ellsworth Mountains and Pensacola Mountains. The Haag Nunataks part of the Ellsworth-Whitmore terrane (EWT) is in yellow. AP, Antarctic Peninsula; TI, Thurston Island.

Fig. 3. Maps of the southeastern part of the Ellsworth-Whitmore terrane and the southwestern part of the Weddell Sea rift system within the Southern Weddell Magnetic Province (Jordan et al., 2017) showing the extent and geological setting of the Pirrit Hills (PH), Nash Hills (NH), Martin Hills (MH) and Pagano Nunatak (PN) granites and associated sub-ice intrusions interpreted from geophysical data from the aerogeophysical survey of Jordan et al. (2013). Data shown are sub-ice topography in panel a, and aeromagnetic data in panel b. Extent of surface outcrop of granite is shown in red, and inferred subsurface extent of granite is shown by the solid white lines. Solid lines indicate the margins of the fault-bounded Transitional Basins (Jordan et al., 2013). Triangles in panel a are subglacial lakes (Smith et al., 2009). Line A - A' is the model crustal cross section shown in Fig. 4.

Fig. 4. 2D potential field model and geological interpretation across the Ellsworth-Whitmore terrane crossing Nash Hills, Martin Hills (MH), the Transitional Basins and the Pagano anomaly (PA). The location of the profile is shown as A - A' in Fig. 3. 4a. Observed and calculated magnetic anomaly (grey dotted line and solid line respectively). 4b. Observed and calculated Bouguer gravity anomaly (grey dotted line and solid line respectively). 4c. Model crustal

structure and depth to source solutions. The model includes upper crust, lower crust, basaltic intrusions at the base of the crust (underplate) and mantle. A thin sediment layer is modelled beneath the Transitional Basins. Magnetic susceptibilities ($\times 10^{-3}$ SI) and densities of the layers and granitic bodies follow Jordan et al. (2013). The long-wave positive gravity anomaly in the centre of the profile is interpreted to result from ~ 3 km crustal thinning across the Transitional Basins as a result of extension. The shorter wavelength negative Bouguer gravity anomalies and positive magnetic anomalies are modelled as 5-8 km thick granite intrusions. Magnetic and gravity data are from aeromagnetic and aerogravity surveys acquired in 2010-2011 (Jordan et al., 2013).

Fig. 5. U-Pb concordia diagram for zircons from Pirrit Hills granite sample V48A. Data point error ellipses are 2σ . Points shown by red ellipses have high U contents of >4000 ppm, are considered to be unreliable and are not included in the age calculation. Points shown by blue ellipses are interpreted to have lost Pb and are also not included in the age. The age of 178.0 ± 3.5 Ma is calculated from the remaining four black solid ellipses.

Fig. 6. Major element variations in the Jurassic Ellsworth-Whitmore terrane granites, oxides in wt.%. The Nash Hills and Martin Hills outcrops are thought to represent the same single granite intrusion, but are shown separately because they show distinct geochemical variations largely as a result of carbonate alteration. Arrows depict approximate trends of increasing MgO and CaO due to carbonate addition to the rocks. Three aplites in the Pirrit Hills, Nash Hills and Pagano Nunataks granites are labelled with a. Data sources: Vennum and Storey (1987), Storey et al. (1988b), Lee et al. (2012), omitting their altered sample P001-1, and new data in this paper.

Fig. 7. Alkali and alkali versus Al variations in the Ellsworth-Whitmore terrane granites compared to Mesozoic granitoids in the Antarctic Peninsula. Intrusions with <59 wt.% SiO_2 not shown. 7a. $\text{K}_2\text{O}/\text{Na}_2\text{O}$ ratio versus SiO_2 . Pagano Nunatak sample V26 and Martin Hills sample

V24 both have K_2O/Na_2O ratios > 2.5 (Storey et al., 1988b) and are interpreted to have been influenced by potassic alteration (trend of alteration depicted by arrow). 7b. molecular $Al/(Ca+Na+K)$ versus SiO_2 . $Al/(Ca+Na+K)$ is aluminium saturation with respect to alkalis and alkali earths; granites with values > 1 are peraluminous, and samples with values < 1 are metaluminous. Data sources: Jurassic Ellsworth-Whitmore terrane granites as in Fig. 6; Antarctic Peninsula granitoids from the data bases of Leat et al. (1995) and Leat et al. (1997) with additional data from Scarrow et al. (1996) and Wever et al. (1995).

Fig. 8. Variation in Ca and trace elements in the Jurassic Ellsworth-Whitmore terrane granites. CaO in wt. %, trace elements in ppm. The Martin Hill sample R.2230.7 is omitted because of evidence it has gained Ca and Sr during carbonate alteration. Plotted trace element data are by ICP-MS. Data are from this paper and Lee et al., (2012). La_N/Yb_N is chondrite-normalised. Eu^* is chondrite-normalised $(Sm+Gd)/2$. Chondritic values from Sun and Macdonough (1989).

Fig. 9. Chondrite-normalised multi-element plots for selected samples of the Jurassic Ellsworth-Whitmore terrane granites. The Pirrit Hills samples are shown as a range. Data from this paper and Lee et al. (2012). The calculated composition of average upper continental crust (Rudnick and Gao, 2003) is shown for comparison. Chondritic values from Sun and McDonough (1989).

Fig. 10. Plots of heat producing elements (ppm) versus heat production ($\mu W/m^3$) from data and calculations in Table 3. The Jurassic Ellsworth-Whitmore terrane granites are shown in the large symbols. The average upper continental crust composition is from Rudnick and Gao (2003). Jurassic Mapple Formation rhyolites representing the Chon Aike 'ignimbrite flare-up' in the Antarctic Peninsula, and derived mainly by partially melting hydrated continental crust are shown for comparison. Assumed rock densities are 2.66 g/cm^3 for the Jurassic granites and average upper continental crust and 2.51 g/cm^3 for Mapple Formation volcanics. Average heat production values and U and Th abundances for four granite plutons of the well-documented HHP Cornubian batholith in southwest England shown for comparison as vertical crosses are: D,

Dartmoor; SA, Saint Austell; B, Bodmin; LE, Land's End; C, Carmenellis. Cornubian data are for borehole samples (Webb et al., 1985).

Fig. 11. Model examining magnitude of heat flow anomalies associated with the Ellsworth-Whitmore terrane granites above regional values. 11a. Plot showing possible values of surface heat flow above the granites in relation to a range of values of regional heat flow and the thickness of high heat production granite. Surface heat flow above the granites is shown for thicknesses of the granite layers of 2, 4, 6 and 8 km, consistent with geophysical modelling (Fig. 4). 11b. cartoon crustal cross section indicating parameters. A regional heat flow value (A) will be increased by the presence of the heat-producing granite (B) depending on the thickness (h) of the heat-producing granite. The larger the radius of the granites (r), the smaller proportion of heat will be dissipated by lateral flow. The granites are assumed to form a uppermost crustal layer with constant thicknesses (h) and have heat productions of $5.35 \mu\text{W}/\text{m}^3$, replacing metasediment of the same volume having heat production of $1.65 \mu\text{W}/\text{m}^3$. Heat production within the granites is assumed to be constant with depth. UC, upper crust, LC, lower crust.

Fig. 12. Plot of $^{206}\text{Pb}/^{238}\text{U}$ age of zircon grains versus U abundance in ppm of the grains using data for the Jurassic granites and the Triassic Mount Seelig granites of the Ellsworth-Whitmore terrane. Data from Lee et al. (2012) and Craddock et al. (2017). Both papers provide data for the Pirrit Hills granite, and these are symbolised separately in the figure. The age of compressive deformation in the Gonwanide orogeny (275-260 Ma) determined from Ar-Ar ages of micas in the Cape Fold Belt (Hansma et al., 2016) is indicated by the green column.

Tables

Table 1. Zircon U-Pb ion-microprobe geochronology for Pirrit Hills granite sample V48A.

Table 2. New chemical analyses for Weddell rift granites.

Table 3. Th, U, K and heat production values (A) (Beardsmore and Cull, 2001) for Weddell rift granites. Original chemical data from Table 1 and Lee et al. (2012).

ACCEPTED MANUSCRIPT

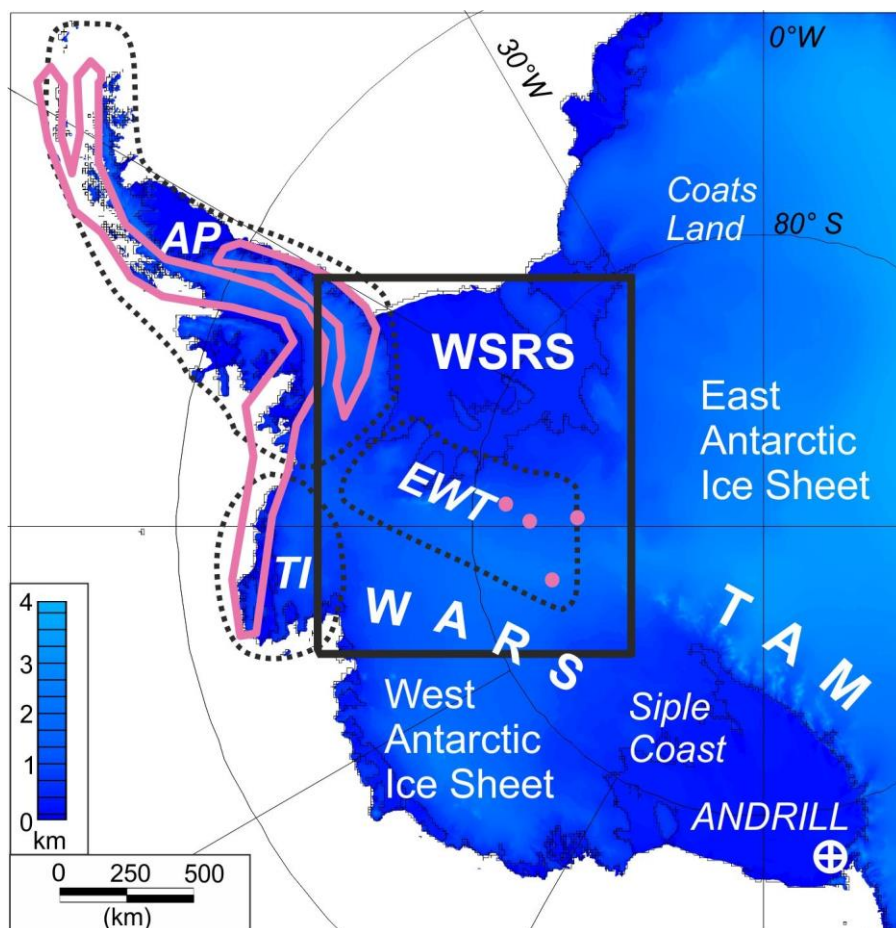


Fig. 1

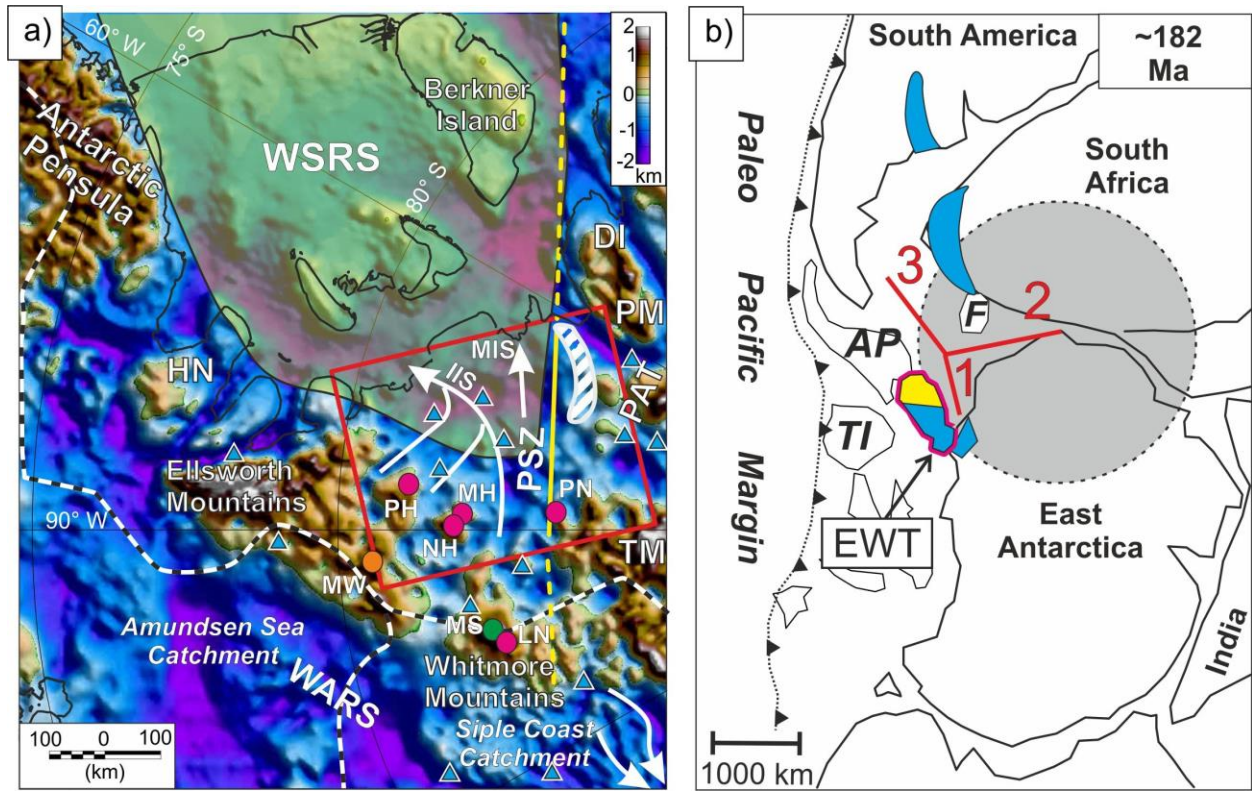


Fig. 2

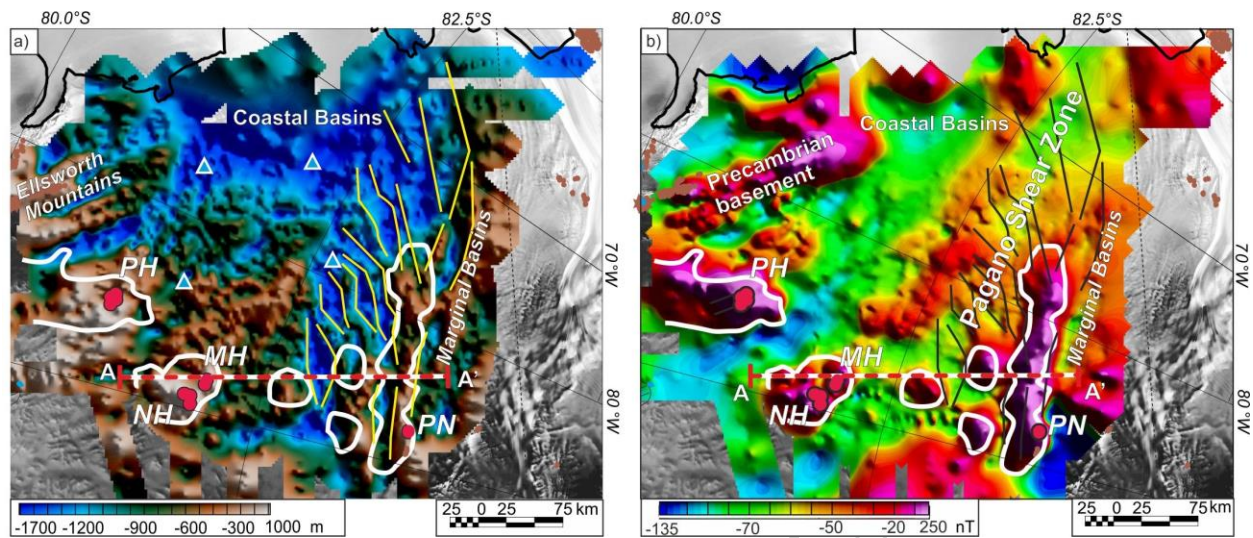


Fig. 3

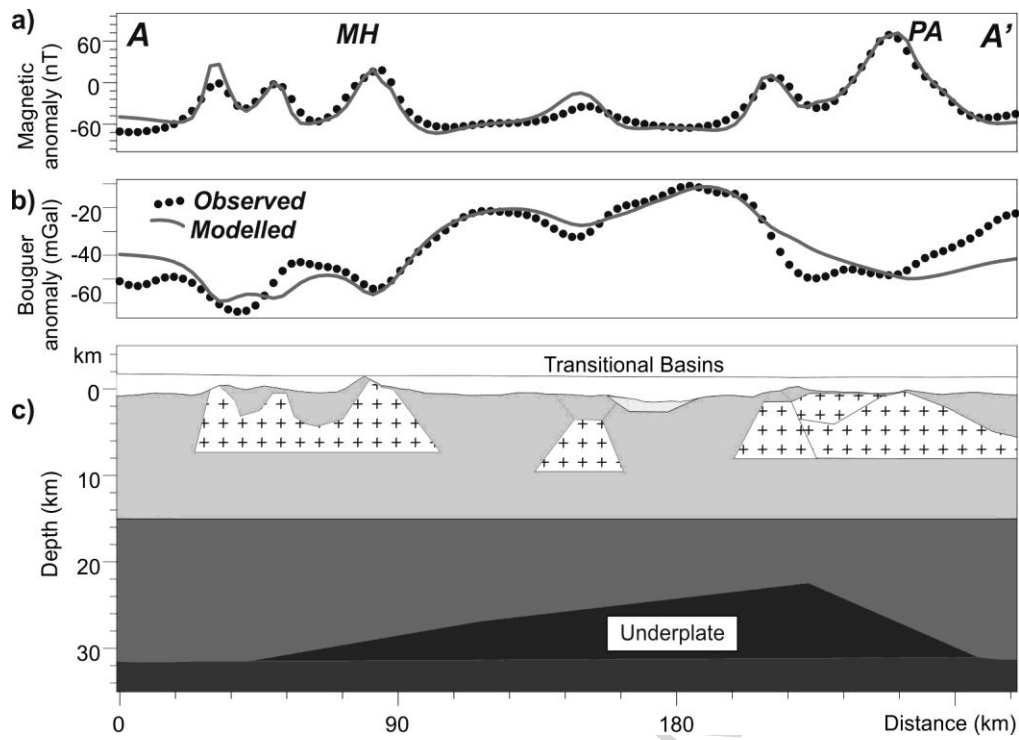


Fig. 4

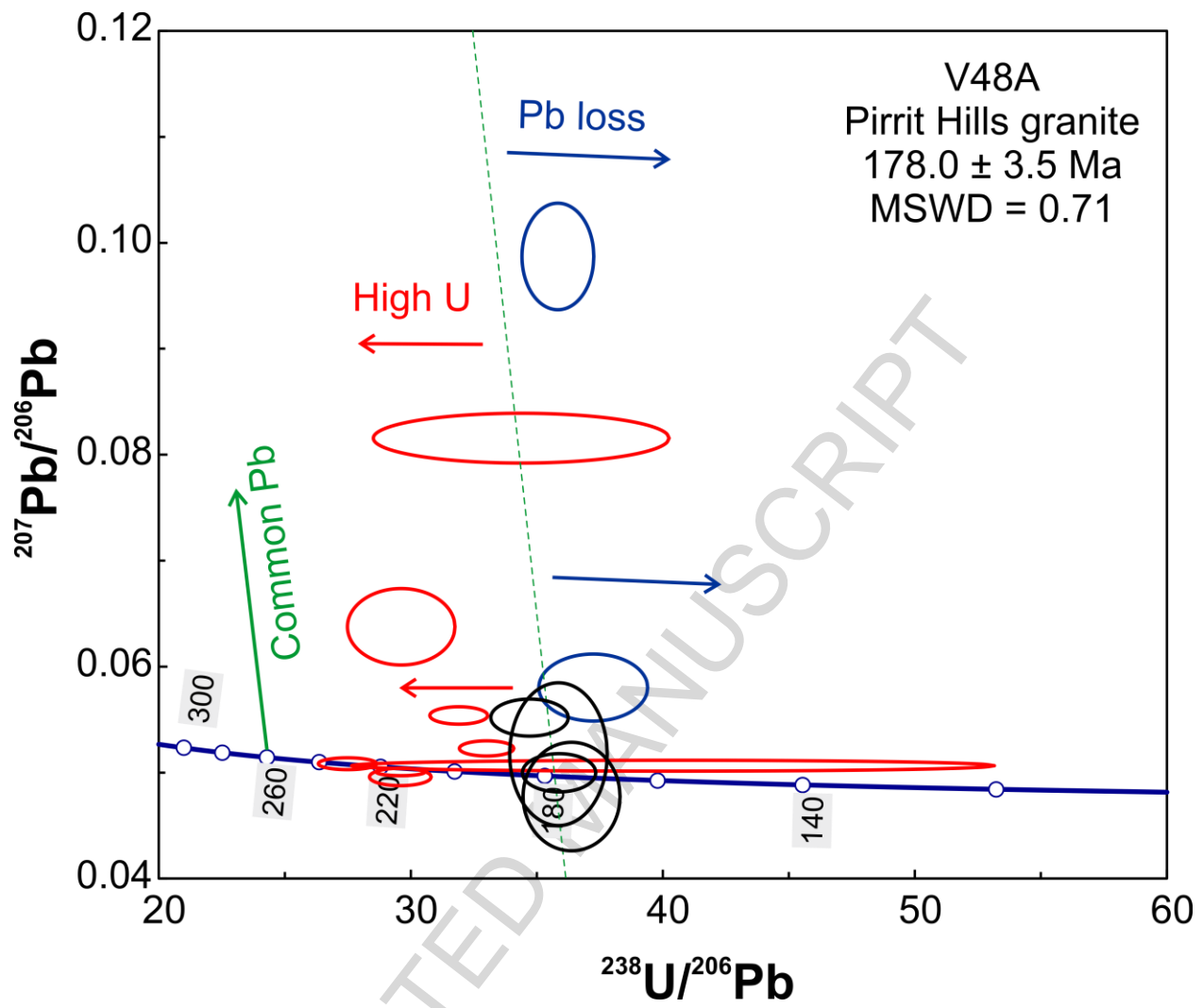


Fig. 5

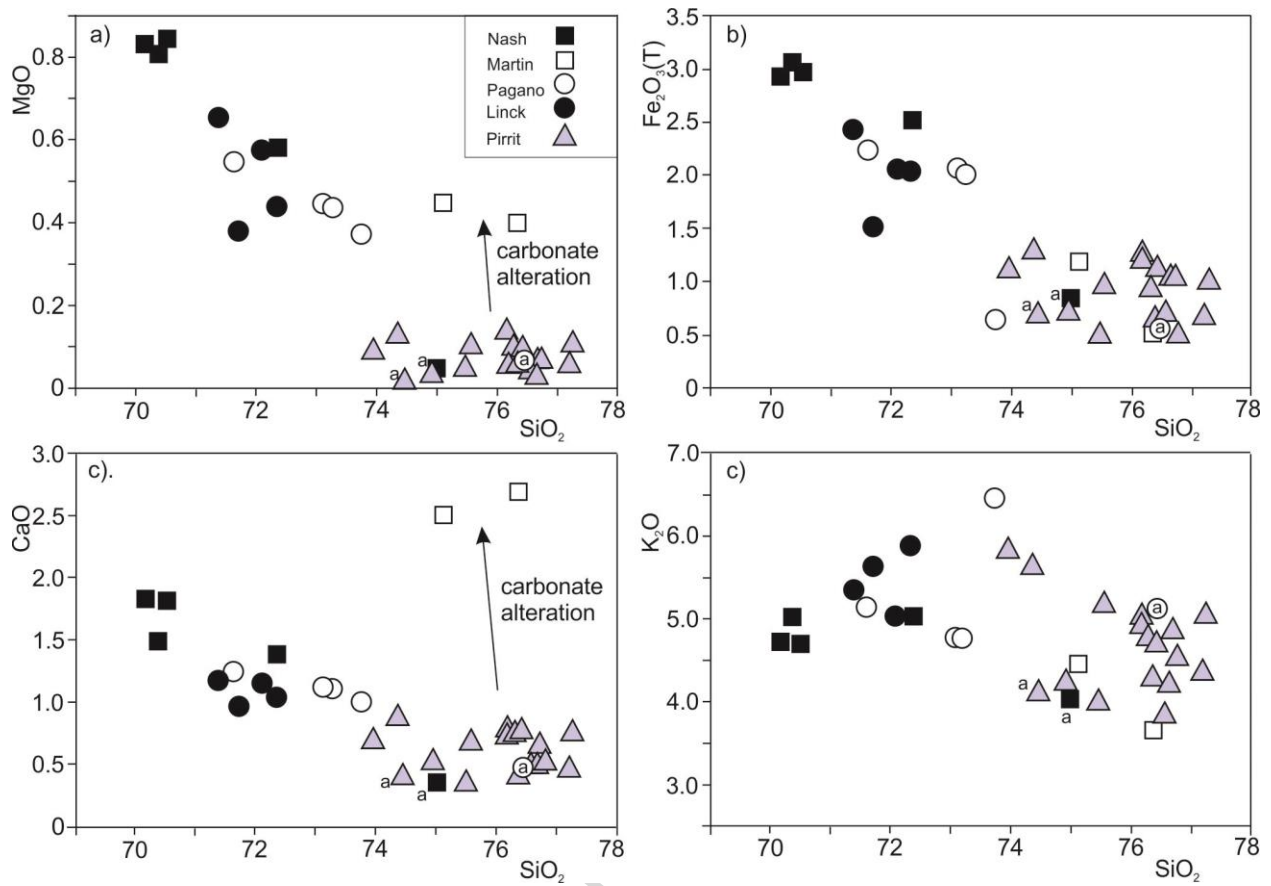


Fig. 6

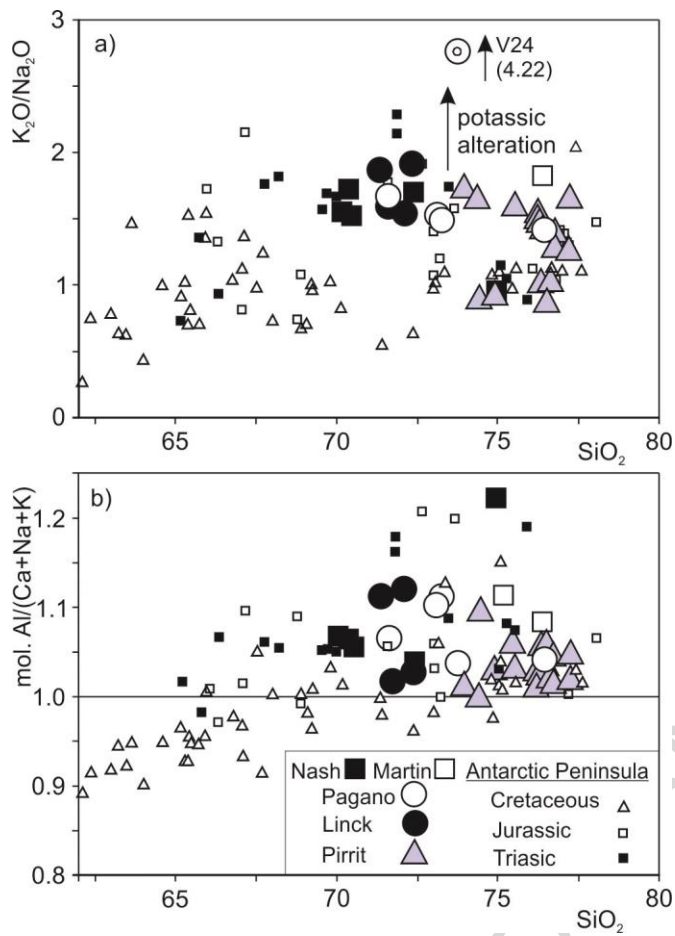


Fig. 7

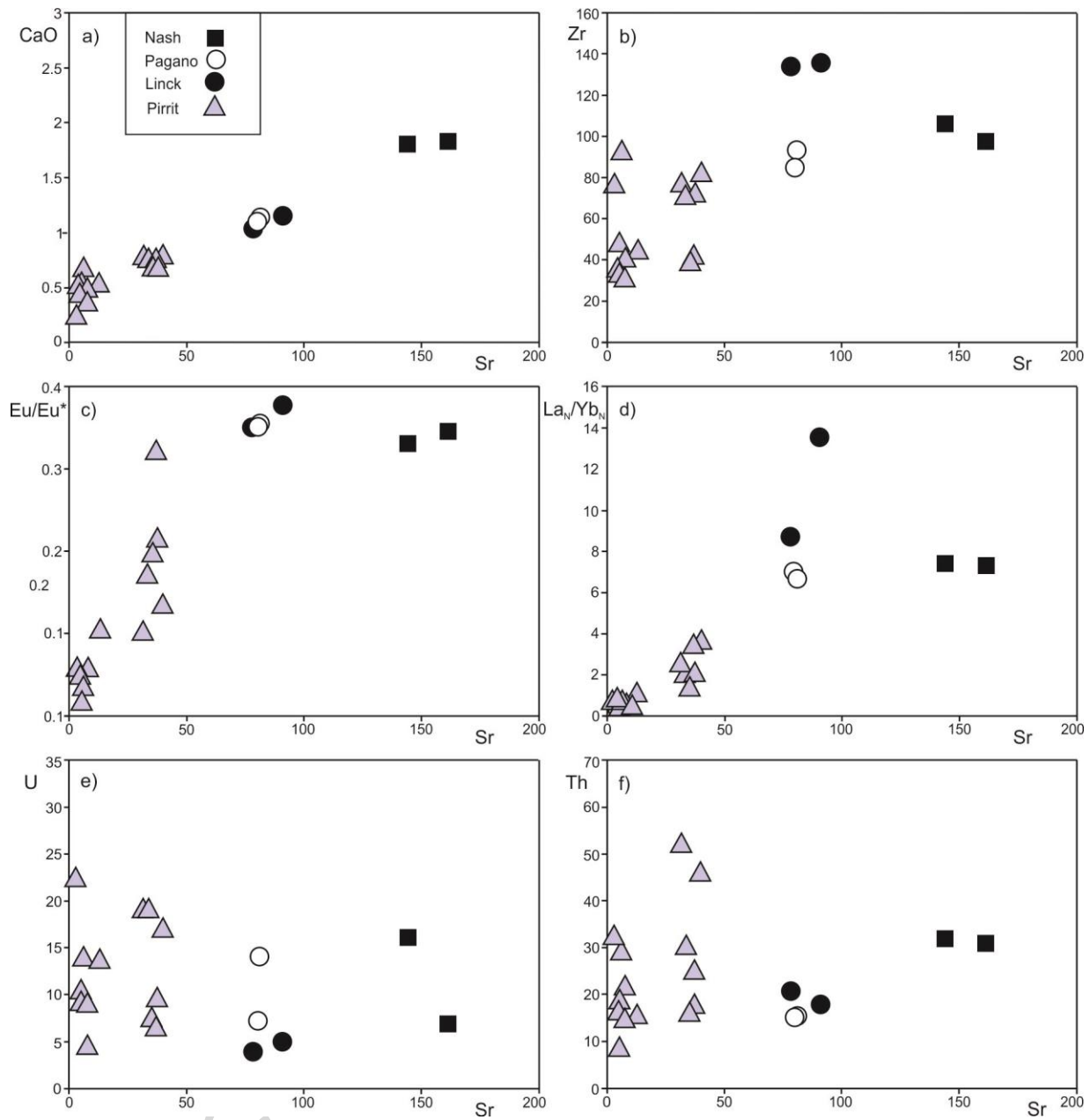


Fig. 8

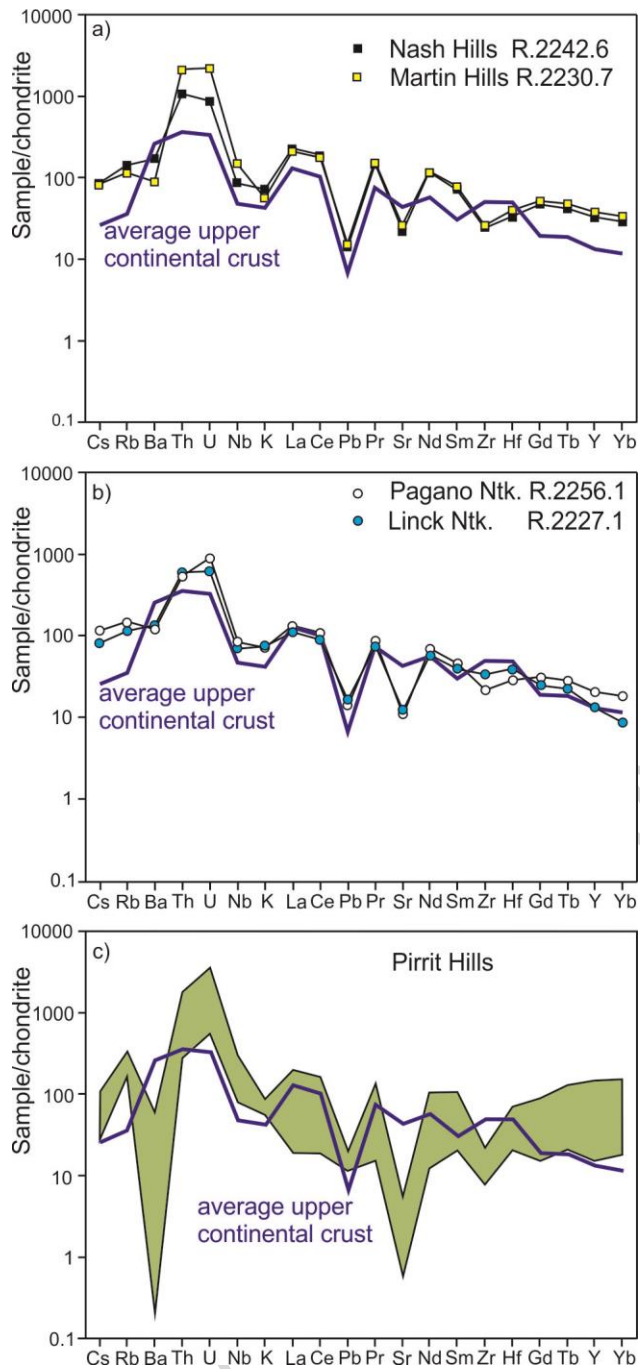


Fig. 9

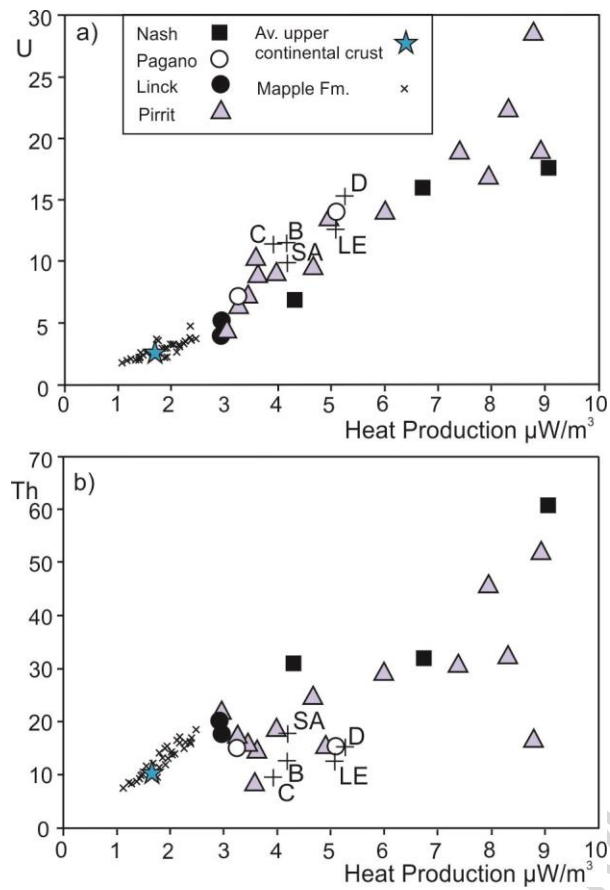


Fig. 10

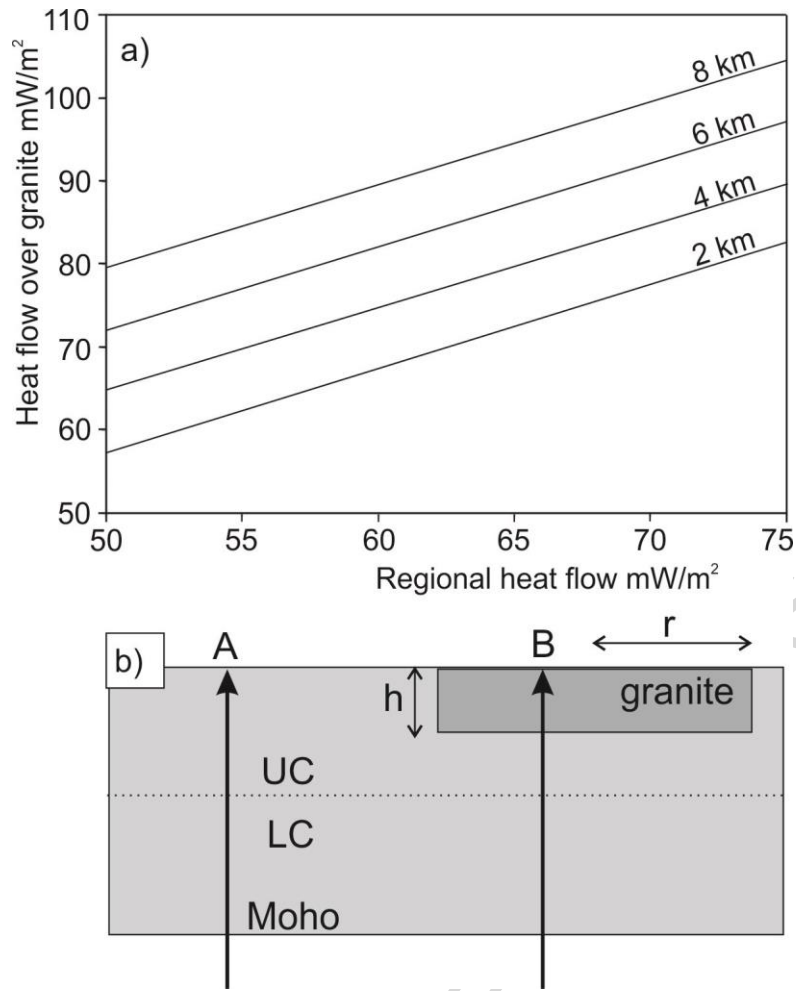


Fig. 11

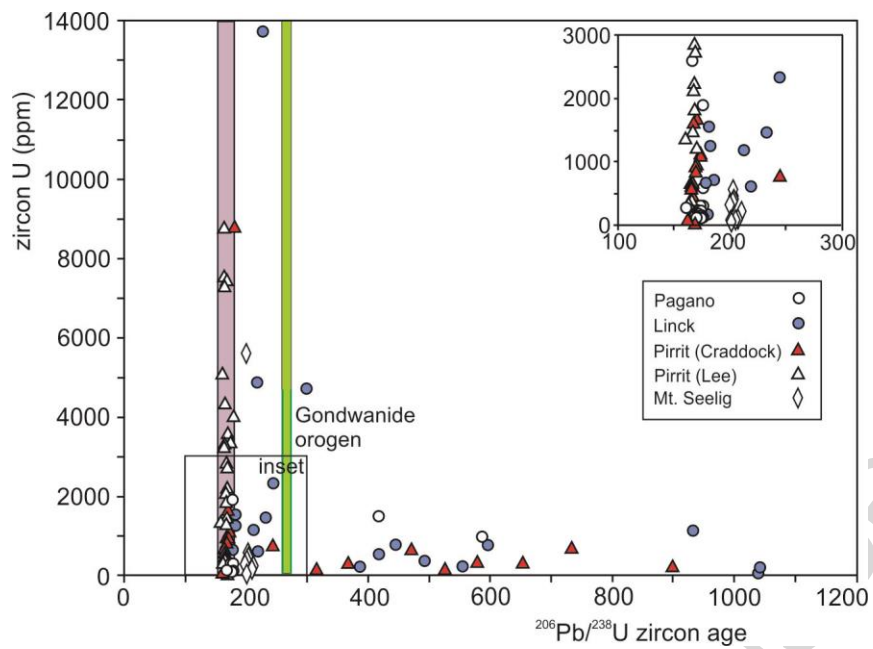


Table 1. Zircon U-Pb ion-microprobe geochronology for Pirrit Hills granite sample V48A

Spot ¹	U (ppm)	Th (ppm)	Pb (ppm)	Th/U	f ²⁰⁶ (%) ²	²³⁸ U/ ²⁰⁶ Pb	±σ (%)	²⁰⁷ Pb/ ²⁰⁶ Pb	±σ (%)	²⁰⁷ Pb/ ²⁰⁶ Pb Pb age (Ma)	±σ	²⁰⁶ Pb/ ²³⁸ U age (Ma)	±σ
9**	91	68	3	0.75	1.21	36.380	2.16	0.04774	4.38	86.3	100.7	174.8	3.7
10**	139	149	5	1.08	0.94	35.861	2.20	0.05174	5.32	273.9	117.5	177.3	3.9
13**	721	407	25	0.56	0.15	35.885	1.66	0.04998	1.47	194.2	33.9	177.2	2.9
7**	2224	1186	78	0.53	0.70	34.713	1.81	0.05519	1.30	419.9	28.7	183.1	3.3
1	17547	1140	635	0.06	0.05	29.599	1.33	0.05005	0.29	197.5	6.6	214.2	2.8
11	4161	1597	144	0.38	0.35	33.010	1.34	0.05228	0.56	297.7	12.7	192.4	2.5
12	7153	592	244	0.08	0.73	31.904	1.47	0.05539	0.61	428.0	13.5	199.0	2.9
14	29551	3772	1171	0.13	0.16	27.492	1.72	0.05084	0.45	233.5	10.3	230.3	3.9
17	8452	2879	327	0.34	0.02	29.587	1.69	0.04959	0.68	175.8	15.8	214.3	3.6
2x	584	625	23	1.07	6.76	35.837	1.62	0.09871	2.08	1599.9	38.3	177.4	2.8
4x	789	1452	53	1.84	22.75	27.907	1.97	0.22647	1.63	3027.3	25.9	227.0	4.4
16x	553	482	19	0.87	0.99	37.241	2.37	0.05803	2.23	530.8	48.0	170.8	4.0
3xx	9277	989	874	0.11	20.66	18.373	9.48	0.21819	11.77	2967.4	178.1	341.6	31.6
5xx	23080	5942	639	0.26	0.10	40.403	12.89	0.05065	0.41	224.9	9.5	157.6	20.1
6xx	32239	28195	1522	0.87	1.41	29.621	2.94	0.06376	2.31	733.8	48.2	214.0	6.2
15xx	23257	14011	825	0.60	4.20	34.384	6.97	0.08156	1.18	1235.0	22.9	184.8	12.7
8 core	95	35	18	0.37	0.00	6.087	2.26	0.07349	1.48	1027.6	29.6	980.6	20.6

1. ** = used in concordia age calculation, x = interpreted to have suffered Pb loss, xx = high U but interpreted to have suffered Pb loss, core = inherited core. 2. Percentage of common Pb detected from the measured ²⁰⁴Pb.

Table 2. Chemical analyses of Ellsworth-Whitmore terrane granites

Sample	R2256.1	R2256.4	R2242.1	R2242.6	R2230.7	R2226.4	R2227.1	R2243.4	R2243.13
Granite	PN	PN	NH	NH	MH	LN	LN	PH	PH
Major elements by XRF (wt.%)									
SiO ₂	73.24	73.11	70.51	70.16	76.36	72.34	72.09	76.43	76.17
TiO ₂	0.29	0.29	0.43	0.43	0.20	0.28	0.30	0.13	0.11
Al ₂ O ₃	13.90	13.73	14.24	14.35	13.22	13.82	14.57	12.54	12.55
Fe ₂ O ₃ (T)	2.00	2.06	2.96	2.91	0.53	2.05	2.07	1.12	1.20
MnO	0.049	0.047	0.051	0.054	0.027	0.025	0.027	0.066	0.047
MgO	0.44	0.45	0.84	0.83	0.40	0.44	0.58	0.10	0.06
CaO	1.11	1.13	1.81	1.84	2.69	1.05	1.16	0.78	0.78
Na ₂ O	3.22	3.14	3.09	3.05	2.01	3.09	3.28	3.36	3.29
K ₂ O	4.77	4.80	4.70	4.72	3.67	5.91	5.06	4.73	4.92
P ₂ O ₅	0.225	0.232	0.169	0.170	0.047	0.199	0.245	0.019	0.013
LOI	0.70	0.72	0.85	0.88	1.31	0.59	0.57	0.60	0.50
Total	99.96	99.72	99.66	99.39	100.46	99.79	99.96	99.87	99.64
Al sat	1.11	1.10	1.06	1.06	1.08	1.03	1.12	1.04	1.03
Elements by ICP-MS (ppm)									
Sc	4.52	4.63	7.07	6.94	6.69	3.54	3.68	7.06	5.77
Ti	0.28	0.29	0.44	0.43	0.19	0.28	0.30	0.12	0.10
V	12.67	13.38	30.78	29.70	4.89	10.34	13.66	4.12	2.09
Cr	4.04	4.12	12.41	12.91	2.20	3.65	6.41	1.11	0.58
Mn	0.04	0.04	0.05	0.05	0.02	0.02	0.02	0.06	0.04
Co	61.43	80.83	81.56	81.00	78.09	69.61	49.63	88.69	130.5
Ni	2.14	1.84	6.56	7.09	1.13	1.15	2.20	0.41	0.40
Cu	1.75	1.65	4.63	2.88	2.43	2.29	3.50	0.71	0.86
Zn	41.97	45.27	48.43	50.89	40.52	64.45	60.09	18.03	13.57
Ga	20.21	21.07	22.86	22.34	21.53	19.64	20.32	20.02	19.17
Rb	344.0	358.8	346.1	334.9	265.2	278.7	273.3	485.7	404.2
Sr	80.24	81.19	144.2	161.4	184.9	78.38	90.98	39.96	31.54
Y	32.70	35.68	53.72	51.95	60.33	28.83	20.89	94.85	110.4
Zr	84.88	93.22	106.2	97.29	100.4	134.4	136.7	81.88	76.81
Nb	20.72	22.43	21.91	21.40	36.68	16.80	18.14	43.97	75.01
Cs	22.26	23.03	15.55	15.74	15.57	7.25	15.92	20.45	5.81
Ba	296.2	303.0	429.4	417.2	213.6	373.6	354.3	93.13	79.63
La	31.01	31.89	51.78	50.83	53.48	30.69	28.09	47.30	35.78
Ce	66.68	68.06	112.5	110.7	115.1	66.76	59.17	100.9	80.35
Pr	8.34	8.56	14.05	13.96	14.22	8.33	7.36	12.95	10.70
Nd	32.38	33.33	54.51	53.55	53.43	31.92	28.19	49.53	42.96
Sm	7.11	7.28	11.27	11.11	11.80	7.43	6.21	12.61	13.27
Eu	0.79	0.82	1.16	1.21	0.85	0.82	0.73	0.55	0.47
Gd	6.45	6.68	9.83	9.82	10.63	6.45	5.34	12.39	15.21
Tb	1.08	1.12	1.62	1.58	1.80	1.06	0.83	2.33	2.97
Dy	6.02	6.29	9.16	9.14	10.44	5.47	4.14	14.36	18.90
Ho	1.11	1.18	1.78	1.81	2.07	0.97	0.71	2.98	4.01
Er	2.98	3.15	4.87	4.88	5.69	2.48	1.68	8.53	11.05
Tm	0.52	0.55	0.83	0.84	0.96	0.42	0.26	1.51	1.81
Yb	3.15	3.41	5.00	5.01	5.62	2.50	1.48	9.40	10.23
Lu	0.51	0.54	0.79	0.79	0.88	0.40	0.23	1.49	1.52
Hf	3.08	3.35	3.70	3.46	4.30	4.48	4.28	3.61	3.53
Pb	35.46	35.19	33.90	35.23	36.28	49.39	40.90	34.05	33.02
Th	15.28	15.49	31.99	31.02	60.70	21.01	18.05	45.79	51.91
U	7.19	14.11	16.06	6.87	17.61	4.03	5.15	16.99	19.11

Granite: PN, Pagano Nunatak; NH, Nash Hills; MH, Martin Hills; LN, Linck Nunatak; PH, Pirrit Hills. Al sat; molecular Al/(Na+K+Ca).

Table 3. Heat Production A(Total) in $\mu\text{W}/\text{m}^3$ and contributions from U, Th and K for Ellsworth-Whitmore terrane granites

Sample	Granite	Source	U ppm	Th ppm	K%	A(U)	A(Th)	A(K)	A (Total)
R2256.1	PN	1	7.19	15.28	3.96	1.85	1.07	0.37	3.29
R2256.4	PN	1	14.11	15.49	3.98	3.63	1.08	0.37	5.08
R2242.1	NH	1	16.06	31.99	3.91	4.13	2.24	0.36	6.73
R2242.6	NH	1	6.87	31.02	3.91	1.77	2.17	0.36	4.30
R2230.7	MH	1	17.61	60.70	3.04	4.53	4.25	0.28	9.06
R2226.4	LN	1	4.03	21.01	4.91	1.04	1.47	0.46	2.96
R2227.1	LN	1	5.15	18.05	4.20	1.32	1.26	0.39	2.98
R2243.4	PH	1	16.99	45.79	3.93	4.37	3.20	0.37	7.94
R2243.13	PH	1	19.11	51.91	4.09	4.92	3.63	0.38	8.93
P001	PH	2	14.0	28.9	4.05	3.60	2.02	0.38	6.00
P001-1	PH	2	22.4	32.2	3.25	5.76	2.25	0.30	8.32
P002	PH	2	13.6	15.5	3.79	3.50	1.08	0.35	4.94
P003-1	PH	2	10.4	8.5	3.56	2.68	0.59	0.33	3.60
P003-2	PH	2	9.2	18.5	3.51	2.37	1.29	0.33	3.99
P004	PH	2	9.6	24.8	4.86	2.47	1.73	0.45	4.66
P005-1	PH	2	4.5	21.3	3.63	1.16	1.49	0.34	2.99
P005-2	PH	2	9.0	14.5	3.33	2.31	1.01	0.31	3.64
P006	PH	2	19.0	30.4	4.20	4.89	2.13	0.39	7.41
P007-1	PH	2	7.4	16.0	4.31	1.90	1.12	0.40	3.42
P007-2	PH	2	28.6	16.3	3.18	7.36	1.14	0.30	8.79
P008	PH	2	6.5	17.4	3.97	1.67	1.22	0.37	3.26

Density of $2660 \text{ kg}/\text{m}^3$ assumed for all samples

Granite: PN, Pagano Nunatak; NH, Nash Hills, MH, Martin Hills; LN, Linck Nunataks; PH, Pirrit Hills

Source: 1, Table 1; 2, Lee et al. (2012)

Highlights

Jurassic granites in the Antarctic Ellsworth-Whitmore terrane have high heat production

Thicknesses and extents of the granites are modelled from aerogeophysical data

The granites generate heat flow anomalies above regional values

The high heat flow may have affected glaciological processes

U enrichment of the source originated during the Gondwanide orogeny

ACCEPTED MANUSCRIPT